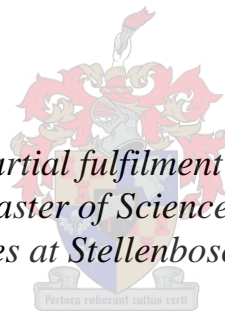# Characterisation of microRNA expression profiles of *Vitis vinifera* in response to grapevine leafroll-associated virus 3 infection

by
Dirk Jacobus Aldrich

Thesis presented in partial fulfilment of the requirements for the degree of Master of Science in the Faculty of AgriSciences at Stellenbosch University

Supervisor: Dr. H.J. Maree

Co-supervisor: Prof. J.T. Burger

March 2017

Declaration

By submitting this thesis electronically, I declare that the entirety of the work contained therein is my own, original work, that I am the sole author thereof (save to the extent explicitly otherwise stated), that reproduction and publication thereof by Stellenbosch University will not infringe any third party rights and that I have not previously in its entirety or in part submitted it for obtaining any qualification.

Dirk Aldrich
March 2017

Abstract

Grapevine leafroll disease (GLD) is endemic to all grape-growing regions of the world and is considered the most significant grapevine viral disease. Grapevine leafroll-associated virus 3 (GLRaV-3) is considered the primary cause of GLD and in South African vineyards five genetic variant groups (I, II, III, VI and VII) have been confirmed. Small RNAs (sRNAs) have been shown to play a significant role in a plant's response to biotic and abiotic stress. This has led to a growing interest in evaluating sRNAs, such as microRNAs (miRNAs), for their role in mediating gene regulation in response to virus infections. In this study, stem-loop RT-qPCR probe-based assays were utilised for miRNA quantitation in GLRaV-3 positive and negative grapevines. A set of own-rooted Cabernet Sauvignon plants representing GLRaV-3 variant groups I, II, III and VI has been established from cuttings of highly symptomatic GLRaV-3 infections found in commercial vineyards. These plants were sampled and screened to yield the first data set. Additionally, young Cabernet Sauvignon plants were established and graft-inoculated with single infections of the five known variants of GLRaV-3 found in South African vineyards. All these plants were maintained in a climate-controlled greenhouse and sampled twice, six months apart, to yield two data sets. A fourth data set comprised of GLRaV-3 positive and negative Cabernet Sauvignon plants sampled from various vineyards in Stellenbosch. Eleven miRNAs were quantified in both infected and healthy grapevine samples. Putative miRNA targets were predicted and annotated using *in silico* analyses. These targets were subsequently quantified in both greenhouse and field samples using a SYBR Green RT-qPCR assay. This study validated statistically significant differences in virus concentrations, expressed as virus concentration ratios (VCRs), in plants singly infected with different GLRaV-3 variants. Interestingly, no difference in mean VCRs were observed between data sets, despite notable differences in plant age, duration of GLRaV-3 infection, scion/rootstock combination and growing conditions. Several miRNAs showed statistically significant expression modulation between infected and healthy samples. miRNA expression between data sets varied substantially and a greater miRNA/target response was observed in plants with more established GLRaV-3 infections. The lack of significant differences in mean VCRs between data sets, coupled with the consistent modulation of certain miRNAs in plants that have likely been infected for longer is a promising result. This finding could indicate that successful inhibition of further virus replication by plant defence mechanisms occurred and that these miRNAs and their targets are implicated in this response. The predicted targets for these miRNAs are genes involved in disease resistance, apoplastic processes, oxidation-reduction processes and growth and developmental processes. Additionally, possible variant-specific miRNA responses to infection were observed across all data sets, which could aid in elucidating possible biological differences between variants of GLRaV-3.

Opsomming

Wingerd-rolblaarsiekte (GLD) is endemies tot alle wingerdstreke ter wêreld en word beskou as een van die mees belangrike virussiektes van wingerd. Grapevine leafroll-associated virus 3 (GLRaV-3) word beskou as die primêre oorsaak van GLD en vyf genetiese variante (I, II, III, VI en VII) van hierdie virus is bevestig in Suid-Afrikaanse wingerde. Verskeie studies het al getoon dat klein RNAs (sRNAs) 'n belangrike rol speel in plantverdedigingsmeganismes teen biotiese en abiotiese stresfaktore. Die betrokkenheid van sRNAs in hierdie verband het gelei tot 'n toename in navorsing gerig tot die karakterisering van uitdrukkingspatrone van sRNAs, insluitend mikroRNAs (miRNAs), en die rol wat hierdie molekule speel in die onderliggende geenregulering in plant virussiektes. Hierdie studie het gebruik gemaak van stam-lus tru-transkripsie kwantitatiewe polimerase kettingreaksie (stem-loop RT-qPCR) om miRNA uitrukking in GLRaV-3 geïnfekteerde- en gesonde wingerdstokke te bepaal. 'n Stel eie-gewortelde Cabernet Sauvignon plante, verteenwoordigend van variantgroepe I, II, III en VI is gevestig vanaf steggies van hoogs-simptomaties plante vanuit kommersiële wingerde. Hierdie plante is gekarakteriseer om die eerste datastel te lewer. Jong Cabernet Sauvignon plante is addisioneel gevestig en geënt met enkel-variant infeksies van die vyf erkende variante van GLRaV-3 in Suid-Afrika. Al hierdie plante is onderhou in 'n klimaatgekontroleerde glashuis en twee maal gekarakteriseer, ses maande uit mekaar, om twee datastelle te lewer. 'n Vierde datastel het bestaan uit GLRaV-3-positiewe en –negatiewe Cabernet Sauvignon plante vanuit kommersiële wingerde in die Stellenbosch omgewing. Elf miRNAs is geïdentifiseer in beide geïnfekteerde en ongeïnfekteerde plantmateriaal. Vermeënde miRNA teikengene is voorspel en geannoteer d.m.v *in silico* analises. Hierdie voorspelde teikengene is daaropvolgend gekwantifiseer in beide glashuis- en veldplante d.m.v 'n SYBR Green RT-qPCR metode. Hierdie studie het statisties-beduidende verskille in viruskonsentrasie, uitgedruk as virus konsentrasie verhoudings (VCRs) tussen plante geïnfekteer met enkele variantgroepe gevalideer. 'n Interessante bevinding is die afwesigheid van beduidende verskille in gemiddelede VCRs tussen datastelle, ten spyte van merkbare verskille in plant ouderdom, tydperk van GLRaV-3 besmetting, bostok/onderstok kombinasies en groei-omstandighede. Verskeie miRNAs het statisties-beduidende verskille tussen geïnfekteerde en gesonde plante getoon. Die miRNA-uitdrukking tussen datastelle het ook aansienlik verskil en 'n meer prominente miRNA/teikengeen respons is gemerk in plante met 'n meer gevestigde infeksie van GLRaV-3. Die afwesigheid van beduidende verskille in gemiddelde VCRs tussen datastelle tesame met die konsekwente modulasie van sekere miRNAs in plante met meer gevestigde GLRaV-3 infeksie is 'n bemoedigende resultaat. Hierdie bevinding kan impliseer dat plantverdedigingsmeganismes suksesvol was in die inhibering van verder virusreplikasie oor tyd en dat hierdie miRNAs en hul teikengene betrokke is in hierdie respons. Die voorspelde teikengene

van hierdie miRNAs is betrokke in groei- en ontwikkelingsprosesse, apoplastiese prosesse, oksidasie-reduksie en siekteweerstand. Hierdie studie het ook moontlike variant-spesifieke miRNA uitdrukking geïdentifiseer wat kan bydra tot pogings om moontlike biologiese verskille tussen variante van GLRaV-3 te identifiiseer.

Acknowledgements

I hereby thank the following individuals and institutions for their contributions to this study:

- Dr. R. Bester, for outstanding mentorship, motivation, intellectual input, skills training and guidance over the past three years and for allowing me to be part of her research.
- Dr. H.J. Maree, for leadership, ongoing guidance, supervision, intellectual input and motivation throughout this study.
- Prof. J.T. Burger, for support and guidance, and for the opportunity to form part of the Vitis laboratory research group.
- All members of the Vitis laboratory.
- Family and friends.
- Vititec, for supplying plant material.
- Stellenbosch University.
- The German Academic Exchange Service (DAAD) for personal funding.
- The financial assistance of the National Research Foundation (NRF) towards this research is hereby acknowledged. Opinions expressed and conclusions arrived at, are those of the authors and are not necessarily to be attributable to the NRF.

Table of Contents

List of figures:

List of tables:

x

List of abbreviations:

AGO	Argonaut
CDS	coding sequence
Cq	Quantitation cycle
CR	Concentration ratio
cv.	Cultivar
DCL1	Dicer-like
dsRNA	double-stranded RNA
EF1α	Elongation factor 1-alpha
ELISA	Enzyme-linked immunosorbent assay
GAPDH	Glyceraldehyde 3-phosphate dehydrogenase
GDP	Gross domestic product
GLD	Grapevine leafroll disease
GLRaV-3	Grapevine leafroll-associated virus 3
GO	Gene ontology
HYL1	Hyponastic Leaves
IDT	Integrated DNA Technologies
miRNA	MicroRNA
mRNA	Messenger RNA
NGS	Next-generation sequencing
no-RT	"no-reverse transcription"
NTC	"no-template" control
OIV	Organisation of Vine and Wine
ORF	Open reading frame
r^2	correlation coefficient
RISC	RNA induced silencing complex
RNAi	RNA interference
ROS	Reactive oxygen species
RT	Reverse transcription
RT-PCR	Reverse transcription polymerase chain reaction
RT-qPCR	Quantitative reverse transcription polymerase chain reaction
SAWIS	South African Wine Industry Information and Systems
SE	Serrate
siRNA	Small interfering RNA
SPL	squamosa promotor-binding-protein-like
sRNAs	Small RNAs
T_A	Annealing temperature
TAE	Tris-acetate-EDTA
UBC	Ubiquitin-conjugating enzyme
UPE	Maximum energy
VCR	Virus concentration ratio
vvi-miRNAs	*Vitis vinifera* microRNAs
α-Tub	alpha-Tubulin

Chapter 1: Introduction

1.1 Background

Grapevine is one of the most widely cultivated fruit crops internationally and has significant economic and agricultural value (Naidu *et al*., 2014). In the South African context, the wine industry is a major contributor to the gross domestic product (GDP), contributing more than R36 billion in total, according to the latest statistics from the South African Wine Industry Information and Systems (SAWIS). Nine wine producing regions have been identified, of which Stellenbosch, Paarl and Robertson are the most prominent in terms of hectares of wine grape vineyards per region (SAWIS). The South African wine industry also contributes significantly to global wine production. The most recent statistics (7 July 2016) from the Organisation of Vine and Wine (OIV) place South Africa as the eighth largest wine-producing country in the world.

Grapevine is susceptible to attack by multiple pathogens including viruses, viroids and phytoplamsas (Naidu *et al*., 2014). Internationally, more viruses have been identified in grapevine than any other fruit crop (Martelli, 2014). Diseases caused by the various virus infections of grapevine can be divided into five major viral disease complexes, of which grapevine leafroll disease (GLD) is considered the most economically important (Atallah *et al*., 2012; Almeida *et al*., 2013; Maree *et al*., 2013 and Naidu *et al*., 2014). GLD significantly impairs overall plant health, with negative effects such as decline in plant vigour and lifespan, disruption of phloem, reduction of crop yield and quality (Cabaleiro *et al*., 1999, Naidu *et al*., 2014; Alabi *et al*., 2016).

Several virus species in the family *Closteroviridae* contribute to GLD etiology, of which *Grapevine leafroll-associated virus 3* (GLRaV-3) is considered the primary causative agent (Maree *et al*., 2013). Eight genetic variant groups of GLRaV-3 have been identified internationally (Ling *et al*., 2004; Engel *et al*., 2008; Maree *et al*., 2008; Jooste *et al*., 2010; Gouveia *et al*., 2011; Bester *et al*., 2012a, Maree *et al*., 2015). To date five of these variant groups (I, II, III, VI and VII) have been identified in South African vineyards (Maree *et al*., 2008; Jooste *et al*., 2011; Jooste *et al*., 2012; Bester *et al*., 2012a; Goszczynski, 2013; Jooste *et al*., 2015, Maree *et al*., 2015). A survey by Jooste *et al.* (2012) showed GLRaV-3 to be the most prevalent virus in South African vineyards.

Limited studies have focussed on characterising the molecular basis of plant-pathogen interactions in GLRaV-3 infection. Plant small RNAs, such as microRNAs (miRNAs), play a crucial role in virtually all aspects of plant growth and development (Chuck and O'Connor 2010), as well as mediate stress

responses to environmental factors (Guleria *et al*., 2011; Khraiwesh *et al*., 2012; Sunkar *et al*., 2012). MicroRNAs negatively regulate the expression of target genes through cleaving of target mRNA (Guleria *et al*., 2011; Khraiwesh *et al*., 2012) or via transcriptional/translational repression (Guleria *et al*., 2011). Investigating biotic stress-responsive miRNA expression and evaluating the expression of their predicted target genes in GLRaV-3 may yield valuable insights into the molecular mechanisms of the GLRaV-3 stress response.

1.2 Problem statement

Grapevine leafroll disease has been recognised as a potential threat to the viticulture industry for several decades, yet our knowledge of the disease remains limited due to the complex nature of its etiology and contrasting symptom expression in red- and white-fruited cultivars (Naidu *et al*., 2014). Gaining knowledge of the molecular mechanisms underlying GLRaV-3 infection remains a high priority. Several genetic variants of GLRaV-3 have been identified internationally, and there is growing evidence that these variants are biologically distinct. Recent findings from around the world indicate that some variants are more prevalent than others in screened vineyards (Sharma *et al*., 2011; Jooste *et al*. 2011; Farooq *et al*., 2013; Chooi *et al*., 2013a; Jooste *et al*., 2015). This may point toward differences in the efficiency of virus variants to infect host plants and spread within and between vineyards. The validation and characterisation of such differences at the molecular level is an essential next step in understanding GLRaV-3 infection, and the contribution of the different variants to GLD etiology.

MicroRNAs have been shown to regulate gene expression in various plant stress responses (Reinhart *et al*. 2002; Khraiwesh *et al*. 2012; Sunkar *et al*. 2012). Several studies have reported differential miRNA expression in plants with viral infections (Bazzini *et al*., 2007; Tagami *et al*., 2007, Alabi *et al*., 2012; Kullan *et al*., 2015). Alabi *et al*. (2012) identified differentially expressed miRNAs in GLRaV-3 infected plants using next-generation sequencing, thereby providing a useful resource for subsequent plant-pathogen interaction studies in GLRaV-3 infection. Additionally, the characterisation of miRNA expression profiles could show a correlation with differences observed in virus concentration and prevalence of certain variants observed in screened vineyards. This data could facilitate further host-pathogen interaction studies, with specific reference to the genetic variability of GLRaV-3. This could also ultimately aid in the development of more targeted GLRaV-3 and GLD intervention strategies.

1.3 Aim and objectives

This study aimed to characterise microRNA expression profiles of *Vitis vinifera* in response to different variant groups of grapevine leafroll-associated virus 3. To achieve this goal, the following objectives were set out:

- To establish single GLRaV-3 variant infected plants under greenhouse conditions using graft-inoculations.
- To collect GLD symptomatic and asymptomatic plant material from commercial vineyards.
- To perform relative quantitation of GLRaV-3 concentration in plants infected with five genetic variants of the virus using a SYBR green RT-qPCR assay.
- To identify miRNAs involved in host-pathogen interactions using previous studies.
- To generate microRNA expression profiles, using probe-based stem-loop RT-qPCR.
- To predict putative miRNA targets using bioinformatic analysis.
- To generate gene expression profiles using SYBR Green RT-qPCR for putative miRNA target genes.
- To evaluate expression profiles of miRNAs and associated targets in greenhouse plants versus field plants.

1.4 Research outputs

Publications and conference proceedings that this study contributed towards are listed below.

1.4.1 Publications

Bester, R., Pepler, P. T., Aldrich, D. J. and Maree, H. J. (2017) Harbin: A quantitation PCR analysis tool. *Biotechnol. Lett*. **39**(1):171-178

1.4.2 Conference Proceedings (Person responsible for presenting is underlined)

- <u>Aldrich DJ</u>, Bester R, Burger JT, Maree HJ. Characterisation of Micro-RNA expression profiles of *Vitis vinifera* in response to Grapevine leafroll-associated virus 3 infection. Virology Africa, 30 November - 3 December 2015 (Cape Town, South Africa) P79 (Poster)

- Bester R, Pepler PT, Aldrich DJ, Maree HJ. Harbin: An analysis tool for relative quantitation of real-time qPCR data and a quantile-based bootstrap test for data pooling. Advances in plant virology, 7-9 September 2016 (Greenwich, United Kingdom) (Poster)

- Aldrich DJ, Bester R, Burger JT, Maree HJ. A snapshot into microRNA regulation underlying different grapevine leafroll-associated virus 3 variant infections. South African Society for Plant Pathology (SASPP) 50th anniversary conference, 15-19 January 2017 (accepted) (Drakensberg, South Africa) (Oral presentation)

Chapter 2: Literature review

2.1 Grapevine

2.1.1 Cultivation and economical importance

Grapevine, a deciduous woody perennial plant, is one of the most widely cultivated fruit crops internationally. Cultivation of domesticated grapevine species dates back to between 6000 and 8000 years ago (This *et al*., 2006; Myles *et al*., 2011). Grapes are currently mainly produced from cultivars of *Vitis vinifera* (Eurasian grapevine), *Vitis labrusca* (Northeast American grapevine), *Vitis rotundifolia* (South-eastern American grapevine) and *Vitis amurensis* (Asian grapevine) (Naidu *et al*., 2014). Grapevine has significant economic value with a wide range of products from table grapes, wine, raisins, and juice to an array of by-products including seed oils and vinegar (Naidu *et al*., 2014). According to statistics from the Food and Agriculture Organization of the United Nations (FAO, 2012), world grape production in 2010 yielded 68 million metric tons from 7.19 million hectares of cultivated grape-growing land.

2.1.2 Viticulture practice

In the majority of grape-growing regions of the world, cultivars are mostly established as grafted vines. In these vines a specific scion cultivar is grafted onto a particular rootstock genotype. This system can improve survival and vigour of grapevine plants, improve scion biomass, increase fruit quality and also promote ripening earlier in the growing season. Soil-borne pathogens such as nematodes and phylloxera (*Daktulosphaira vitifoliae*) pose a significant threat to the survival of grapevine plants. The use of resistant rootstock genotypes is thus an essential measure to ensure plant survival in regions where these pathogens are found (Jones *et al*., 2009; Naidu *et al*., 2014). Since grapevine is clonally propagated, the establishment of new vineyards with infected plant material and the distribution of infected vegetative cuttings is the primary route for spreading viruses and virus-like pathogens (Demangeat *et al*., 2010, Tsai *et al*., 2012; Naidu *et al*., 2014).

2.1.3 Threats and viral diseases

Over 70 pathogenic agents have been shown to infect grapevine, including viruses, viroids and phytoplasmas. This is the highest abundance of intracellular pathogens found in any fruit crop. (Martelli *et al*., 2014). Diseases caused by the various virus infections of grapevine can be divided

into five major viral disease complexes; grapevine degeneration and decline, graft incompatibility, rugose wood complex, fleck disease complex and grapevine leafroll disease (GLD). (Almeida *et al*., 2013; Maree *et al*., 2013 and Naidu *et al*., 2014).

2.2 Grapevine leafroll disease

Grapevine leafroll disease has been shown to be present in all grape-growing regions of the world (Cabaleiro and Segura, 2006; Maree *et al*., 2008, Almeida *et al*., 2013, Naidu *et al*., 2014, Jooste *et al*., 2015). The substantial economic impact of this disease has led to its status as the most important viral disease affecting grapevine internationally (Freeborough and Burger, 2006; Nimmo-Bell, 2006; Naidu *et al*., 2008; Atallah *et al*., 2012).

2.2.1 Symptomatology and physiological impact

The foliar symptoms of most red-fruited cultivars, as reported by Maree *et al*. (2013), include a downward rolling of leaf borders towards the later stages of the growing season, as well as reddening of interveinal leaf areas. The leaves of white cultivars could become slightly chlorotic, leading to a yellow discolouration that is less pronounced than red-fruited cultivar symptoms (Figure 2.1). Symptom expression can vary significantly and is influenced by various factors. The specific cultivar, combination of virus co-infections, growing season, weather conditions and rootstock/scion combinations are considered key factors influencing symptom expression (Maree *et al.*, 2013; Naidu *et al*., 2014; Naidu *et al*., 2015). The wide range of effects of specific rootstock genotypes on plant growth, grape composition and biotic and abiotic stress response factors are well documented. Effects pertaining to stem-biomass and vigour, sap phenolic levels, abiotic and biotic stress resistance and disease symptom expression have been reported in recent studies (Jensen *et al*., 2010; Cookson and Ollat, 2013; Wallis *et al*., 2013). Accordingly, the effects of GLD in red-fruited cultivars were reported to differ in grafted vines of varying rootstock/scion combinations, with reference to yield loss, vigour and fruit quality (Lee *et al*., 2009; Lee and Martin, 2009; Komar *et al*., 2010; Mannini *et al*., 2012). Although some asymptomatic grapevine varieties have been identified, no natural source of GLD resistance has been found in *V. vinifera* (Weber *et al*., 1993; Martelli, 2000; Naidu *et al*., 2014).

6
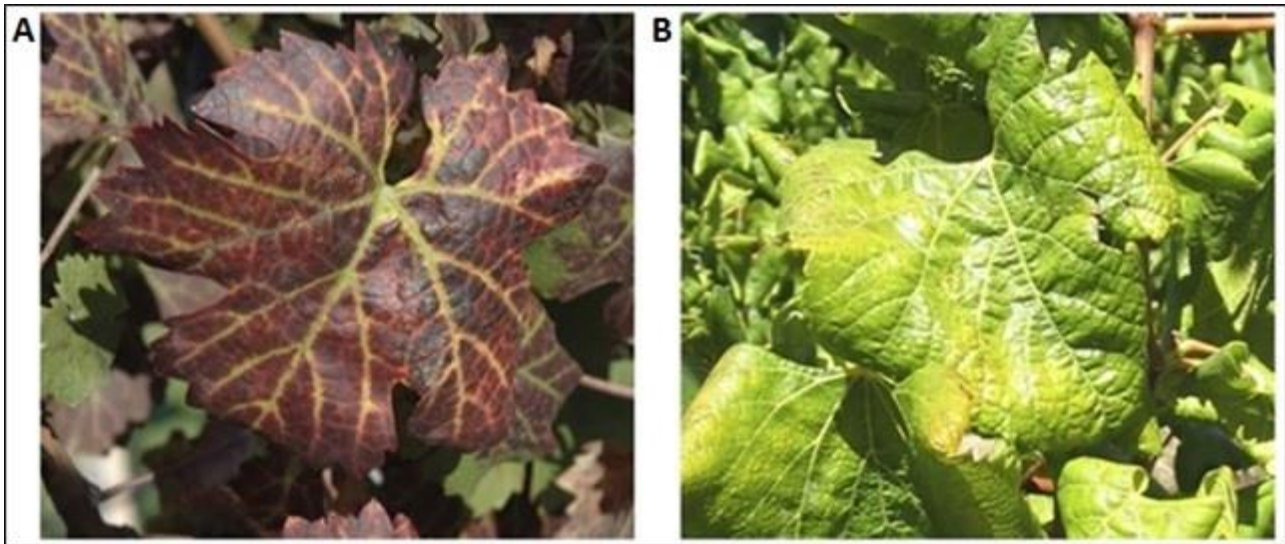
Figure 2.1 Classical GLD symptoms: (A) a red-fruited cultivar (*V. vinifera* cv. Cabernet Franc) and (B) a white-fruited cultivar (*V. vinifera* cv. Chardonnay) (Maree *et al*., 2013).

GLD causes substantial impairment of overall plant health, which includes a reduction in plant vigour and lifespan, disruption of phloem and negatively impacting on crop ripening, quality and yield (Cabaleiro *et al*., 1999, Naidu *et al*., 2014; Alabi *et al*., 2016). This disease negatively affects the production value of grapevine, with special reference to wine making, by decreasing berry sugar and total soluble solids content and increasing the acidity of must (Cabaleiro *et al*., 1999; Martinson *et al*., 2008; Alabi *et al*., 2016).

A distinctive feature of GLD is that symptom expression is usually only apparent on mature leaves during berry ripening (post-véraison) later in the growing season, even though GLRaV-3 is systemically distributed and detectable throughout the entire season (Naidu *et al*., 2015). GLD thus represents a complicated disease system in which symptom expression, or the lack thereof, correlates to two broad physiological cycles, namely pre-véraison (berry formation) and post-véraison (Naidu *et al*., 2015).

2.2.2 Disease management

The need for long term, large-scale management strategies of GLD is emphasised in various case studies from grape-growing regions around the world (Pietersen 2006; Hoskins *et al*., 2011; Sharma *et al*., 2011). Grapevine is a clonally propagated crop and as such the primary means of GLD transmission is through the propagation of infected plant material (Charles *et al*., 2006). Several insect vectors have been shown to also mediate GLD spread, which includes various species of mealybugs

and soft-scale insects (Tsai *et al*., 2008; Charles *et al*., 2009). Infected plant material in vineyards affected by GLD, especially material showing no symptoms, will act as reservoir and aid the spread of the disease (Almeida *et al*., 2013; Maree *et al*., 2013). Therefore, the importance of certification programs to ensure the production of clean propagation material is an integral part of GLD management (Maree *et al*., 2013).

2.3 Grapevine leafroll-associated virus 3

2.3.1 Taxonomy and genome organisation

Grapevine leafroll disease is caused primarily by infection with *Grapevine leafroll-associated virus 3* (GLRaV-3) in the genus *Ampelovirus*. Grapevine leafroll-associated virus 3 forms part of a collection of virus species in the family *Closteroviridae* that contribute to GLD etiology (Martelli *et al*., 2011, 2012; Maree *et al*., 2013). GLRaV-3 is a long, filamentous, monopartite, linear, positive-sense single-stranded RNA virus that is limited to the phloem of host plants (Martelli *et al*., 2002). The genome of GLRaV-3 consists of 11 to 12 open reading frames (ORFs) (Agranovski *et al*., 1994; Ling *et al*., 1998; King *et al*., 2011). Functional annotation of the GLRaV-3 genome has relied mostly on inference of putative ORF functions using homologous genomes of other positive-sense single-stranded RNA viruses (Maree *et al*., 2013)

2.3.2 Virus detection

Grapevine leafroll-associated virus 3 detection in plant material has been achieved with various established techniques including biological indexing, serology, nucleic acid-based methods and next-generation sequencing (NGS). Biological indexing using indicator plants is an effective technique for disease detection, but requires time for symptom expression to manifest and often relies on subjective evaluation by skilled personnel. Additionally, biological indexing does not allow the identification of the specific causative pathogen(s) of a disease (Al Rwahnih *et al*., 2015). Several serological methods of GLRaV-3 have been developed including enzyme-linked immunosorbent assays (ELISA), immunofluorescence and immune strip tests. (Schaad *et al*., 2003). Serological methods such as ELISA are less sensitive than nucleic acid-based methods, but remain a popular method for routine testing in the industry due to their robustness (Maree *et al*., 2013). Nucleic acid-based techniques such as reverse transcription polymerase chain reaction (RT-PCR) and microarrays have been shown to be very successful in GLRaV-3 detection (Engel *et al*., 2010; Bester *et al*., 2012b). These techniques, however, do not take into account the involvement of other known or unknown viruses

in causing disease, and different virus variants could also go undetected in highly specific protocols (Maree *et al*., 2013).

Next-generation sequencing allows for virus detection without previous sequence information and can detect previously unknown viruses. Establishing a total viral complement of a sample, through metagenomic sequencing, has been shown to circumvent the limitations of other plant virus detection methods (Kreuze *et al*., 2009; Coetzee *et al*., 2010). This method is not limited by viral strain differences. Although NGS is a powerful diagnostic tool that allows for the detection of novel viruses and viral variants in grapevine, further biological work is needed to validate and characterise the discovery (Al Rwahnih *et al*., 2015).

2.3.3 Genetic variants

Various recent studies have focused on characterising the genetic variability of GLRaV-3 (Fuchs *et al*., 2009; Gouveia *et al*., 2011; Jooste *et al*., 2010, 2011; Bester *et al*., 2012a; Kumar *et al*., 2012; Seah *et al*., 2012; Sharma *et al*., 2011; Wang *et al*., 2011a; Chooi *et al*., 2013a, 2013b; Farooq *et al*., 2013; Goszczynski, 2013; Liu *et al*., 2013). Fuchs *et al*. (2009) used phylogenetic analysis of the heat shock protein 70h gene to show the existence of at least five genetic variant groups of GLRaV-3. The first complete assembly of the GLRaV-3 genome (isolate GP18 from South Africa) by Maree *et al*. (2008) was an important initial step in allowing full genome comparison of virus isolates to validate the existence of different variants of GLRaV-3. To date, eight genetic variant groups of GLRaV-3 have been identified internationally (Ling *et al*., 2004; Engel *et al*., 2008; Maree *et al*., 2008; Jooste *et al*., 2010; Gouveia *et al*., 2011; Bester *et al*., 2012a, Maree *et al*., 2015). In South African vineyards five of these variant groups namely I, II, III, VI and VII have been detected (Maree *et al*., 2008; Jooste *et al*., 2011; Jooste *et al*., 2012; Bester *et al*., 2012a; Goszczynski, 2013; Jooste *et al*., 2015, Maree *et al*., 2015).

Maree *et al*. (2015) proposed the classification of GLRaV-3 variant groups into four supergroups labelled A to D. Variant groups I to V comprise supergroup A and show the highest degree of sequence identity (above 85%) between GLRaV-3 isolates. Supergroups B, C and D comprise variant groups VI, VII and VIII, respectively. Variants from group VI (supergroup B) have higher genetic diversity compared to supergroup A and have distinct genome characteristics including the absence of ORF2 (Maree *et al*., 2015). Phylogenetic analysis revealed isolate GH24 (variant group VII) to be highly divergent to other known genetic variant groups of GLRaV-3. At the nucleotide level, GH24 also lacks ORF 2 and shares less than 66% sequence identity with any GLRaV-3 isolates comprising

the known variant groups of the virus. (Maree *et al*., 2015). In this study isolates from each of the five variant groups known to be present in South Africa were used, they were isolates 621 (Jooste *et al*., 2010), GP18 (Maree *et al*., 2008), PL-20 (Jooste *et al*., 2010), GH30 (Bester *et al*., 2012a) and GH24 (Maree *et al*., 2015) representing variant groups I, II, III, VI and VII, respectively. No significant difference in symptom expression has been reported between GLRaV-3 variants (Blaisdell *et al*., 2015).

Research aimed at characterising the biological properties of GLRaV-3 variants is an essential next step in further understanding GLRaV-3 infection and GLD etiology. Currently, little is known about possible differences in pathogenicity of these variants, though recent studies have yielded interesting findings. The first evidence of GLRaV-3 variants being biologically distinct was produced by Blaisdell *et al*. (2012), who showed significant differences in transmission efficiency between variant groups I and VI, as tested in the Napa Valley, California. In a recent South African report, Bester *et al*. (2014) found a significant difference in virus concentration ratio (VCR) between plants infected with variant groups II and VI, respectively. Variant group II showed a higher GLRaV-3 concentration when compared to group VI, indicating possible differences in the efficiency of viral infection and replication within the host, between variants of GLRaV-3. In a South African study, Jooste *et al*. (2015) identified variant groups II and VI to be the most abundant in screened samples. A previous survey by Jooste *et al*. (2011) also showed a predominant presence of variant group II in 10 mother blocks in South African vineyards. Additionally, this study showed variant group II to have a faster spread in a disease cluster compared to variant group III. At the time of this survey, variant group VI had not been identified and as such the spread of group VI was not investigated (Jooste *et al*., 2015). The predominant occurrence of variant groups II and VI in the 2015 survey suggests that these variant are more effectively transmitted to neighbouring plants in a disease cluster. Validating such differences at the molecular level is important for furthering our understanding of GLRaV-3 and the possible biological distinctions that can be made between variants of the virus.

2.3.4 Compatible plant-pathogen interaction

Plants are exposed to various stresses, both biotic and abiotic, and have numerous response mechanisms to counter adverse effects (Sunkar *et al*., 2012). These mechanisms are controlled by a complex gene regulation network. Reactive oxygen species (ROS) accumulation in the apoplast is a primary, universal part of plant cell defence against biotic stresses (Bolwell *et al*., 2002; Gutha *et al*., 2010; Sgherri *et al*., 2013). A report by Espinoza *et al*. (2007b) showed up-regulation of defence-related genes in symptomatic leaves, which suggests concomitant activation of host-defence response

and symptom development. The precise mechanism triggering the host defence response to GLRaV-3 has yet to be elucidated. A promising hypothesis is that impairment of electron transport during photosynthesis induces the production of ROS, leading to oxidative stress in symptomatic leaves. Production of ROS could likely trigger the accumulation of anthocyanins observed in symptomatic leaves (Gutha *et al*., 2010), and due to its free radical scavenging capacity (He *et al*., 2010) would serve a protective function against oxidative stress. The reddening of interveinal regions in symptomatic red cultivars could likely be due to this anthocyanin build up (Gutha *et al*., 2010).

The most common physiological effects of GLRaV-3 infection on red-fruited cultivars are related to a disruption of photosynthesis and carbohydrate metabolism (Bertamini and Nedunchezhian, 2002; Basso *et al*., 2010; Gutha *et al*., 2012). Espinoza *et al*. (2007a) evaluated changes in gene expression of two red-fruited cultivars infected with GLRaV-3, using global transcript profiling. Results from this study indicated changes in expression of genes involved in various biological processes, including secondary metabolism, photosynthesis, transcription factors and transport. Bertamini *et al*. (2004) assessed the effect of GLRaV-3 infection on electron transport and found a disruption of the electron transport chain on the donor side of Photosystem II.

2.4 Plant small RNAs

Small RNAs (sRNAs) are involved in both transcriptional and post-transcriptional gene regulation, thereby acting on both RNA (mRNA) and DNA to effect gene regulation. Plant sRNAs play crucial roles in virtually all aspects of plant growth and development (Chuck and O'Connor, 2010) as well as mediate stress responses to environmental factors (Guleria *et al*., 2011). The functions of microRNAs (miRNAs) in plant stress responses are well documented, with various miRNAs having been identified to be involved in specific stresses such as bacterial infection, salinity, drought stress, virus infection and mechanical stress (Reinhart *et al*., 2002; Khraiwesh *et al*., 2012; Sunkar *et al*., 2012). Differential miRNA expression in plant viral infection has been shown in multiple studies (Bazzini *et al*., 2007; Tagami *et al*., 2007, Alabi *et al*., 2012; Kullan *et al*., 2015). Alabi *et al*. (2012) assessed the expression of *V. vinifera* miRNAs (vvi-miRNAs) in GLRaV-3 infected grapevine using NGS. Differential expression of several miRNAs was observed in infected plants, which facilitates subsequent studies aimed at characterising the specific roles of vvi-miRNAs in GLRaV-3 infection and GLD.

2.4.1 Classification and RNA interference

Small RNAs (sRNAs) can be divided into two distinct groups. The two main classes of small RNAs (sRNAs) are small interfering RNAs (siRNAs) and microRNA (miRNAs) (Guleria *et al*., 2011). Small interfering RNAs (21 to 24 nucleotides in length) are produced from long double-stranded RNA (dsRNA) precursors, which can be either endogenous or exogenous in origin (Guleria *et al*., 2011). Endogenous dsRNA originates from various sources, including transcription of inverted repeats, transgenes and other repeat elements (Pantaleo *et al*., 2010). An exogenous source of dsRNA can be the dsRNA replication intermediate of single-stranded RNA viruses (Guleria *et al*., 2011; Triantafilou *et al*., 2012). MicroRNAs are 18-25 nucleotides long (Chen *et al*., 2005) and are transcribed by genes annotated as *MIR* genes (Guleria *et al*., 2011).

Although these groups differ in terms of biogenesis, they share the capacity to associate and bind to Argonaute (AGO) proteins (Axtell *et al*., 2013). These proteins cluster to form the structural and catalytical components of what is known as the RNA induced silencing complex (RISC) (Iwakawa and Tomari, 2015). RISC is the effector mechanism in RNA interference (RNAi), or RNA directed gene regulation, and acts upon target messenger RNA (mRNA) under the direction of sRNA/mRNA complementarity (Guleria *et al*., 2011). RNAi can effect gene regulation at both the transcriptional and post-transcriptional levels by either targeting DNA for methylation, or by cleaving target mRNA (Guleria *et al*., 2011; Khraiwesh *et al*., 2012). Additionally, the RISC complex can cause translational repression by binding to target mRNA and preventing translation by obstructing the actions of ribosomes (Guleria *et al*., 2011).

2.4.2 MicroRNAs

MicroRNAs are the best characterised group of sRNA, even though they are not the most abundant group. Several miRNAs have been reported to play significant roles in regulating genes involved in plant growth and development and both abiotic and biotic stress responses, including viral infection (Bazzini *et al*., 2007; Tagami *et al*., 2007; Alabi *et al*., 2012; Singh *et al*., 2012; Kullan *et al*., 2015). The precursors for miRNAs are endogenous hairpin-shaped, single stranded RNA molecules transcribed from genomic DNA. The nuclear-encoded *MIR* genes are transcribed by RNA polymerase II (RNA pol II) to yield primary miRNA transcripts (pri-miRNAs) that are subsequently processed to generate pre-miRNAs and finally mature miRNAs (Figure 2.2) (Guleria *et al*., 2011; Khraiwesh *et al*., 2012). Dicer-like (DCL1), Hyponastic Leaves 1 (HYL1) and serrate (SE) proteins catalyse the processing of the miRNA precursor into a miRNA duplex, which is subsequently methylated and

exported to the cytoplasm. (Guleria *et al*., 2011; Khraiwesh *et al*., 2012) Pre-miRNAs contain two functional strands, namely the 5′ strand and the 3′ strand. In the pre-miRNA molecule, this is known as the -5p/-3p duplex (previously known as the miRNA/miRNA* duplex). Following processing and transportation to the cytoplasm, one of these strands associates with the RISC complex and guides the process of RNAi under the direction of mRNA/miRNA complementarity (Khraiwesh *et al*., 2012; Sunkar *et al*., 2012). The endonuclease activity of the AGO proteins cleave target mRNA between positions 10 and 11 of the alignment (Axtell *et al*., 2013; Iwakawa and Tomari, 2015).
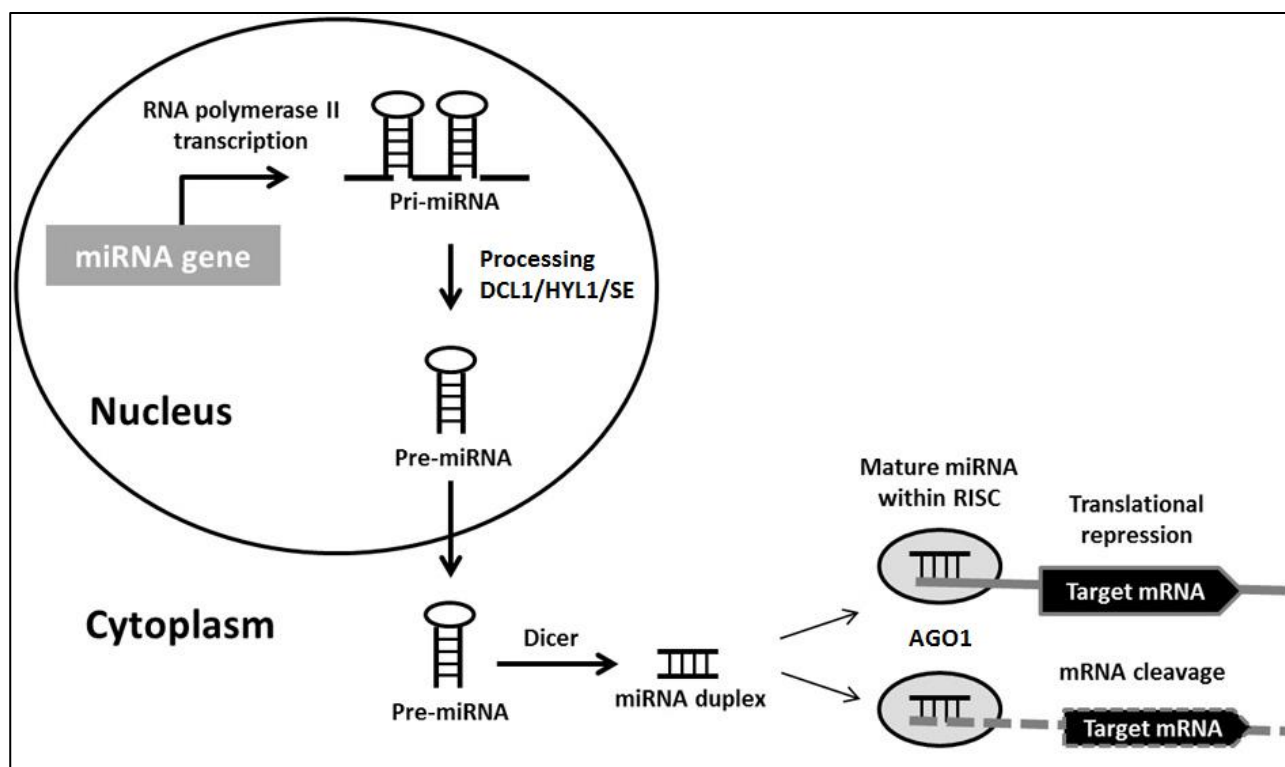
Figure 2.2 Schematic of plant miRNA biogenesis (adapted from Goodall *et al*., 2013)

2.4.3 MicroRNA quantitation

Accurate quantitation of miRNAs poses several challenges owing to their unique characteristics (Wark *et al*., 2008). The roughly 22 nucleotide length of mature miRNAs is too small for conventional PCR primers (Pritchard *et al*., 2012). Additionally, miRNAs lack a consensus sequence, for instance a poly(A) tail, for use in selective enrichment, which is important considering that miRNAs comprise only a small fraction (roughly 1%) of total RNA mass (Pritchard *et al*., 2012). MicroRNAs from the same family can also differ by only a single nucleotide, highlighting the importance of specificity in a quantitation assay (Pritchard *et al*., 2012). Currently, three methods of miRNA quantitation are well-established: quantitative reverse transcription polymerase chain reaction (RT-qPCR),

hybridisation-based approaches (such as microarrays) and next-generation sequencing (NGS) approaches (Pritchard *et al*., 2012). All three approaches have specific advantages and disadvantages pertaining to application, cost, sensitivity and the ability to detect novel miRNAs. These approaches are summarised in a recent review by Pritchard *et al*. (2012).

Chen *et al*. (2005) introduced a sensitive, inexpensive method for miRNA quantitation using stem-loop primers for reverse transcription (RT) of miRNAs followed by TaqMan® PCR analysis (Figure 2.3). These assays are specific to mature miRNAs and have the capacity to distinguish between two related miRNAs differing by as little as one nucleotide. The speed, accuracy and specificity of this assay makes it ideal for miRNA expression profiling (Chen *et al*., 2005). The stem-loop RT primer has several advantages that contribute to assay specificity. Base stacking in the stem-loop region to improve thermal stability, and spatial constraint of the primer structure that allows for more specific binding to target miRNAs (Chen *et al*., 2005). In addition, this assay can also be used to quantitate the expression of other sRNAs such as siRNA (Chen *et al*., 2005).
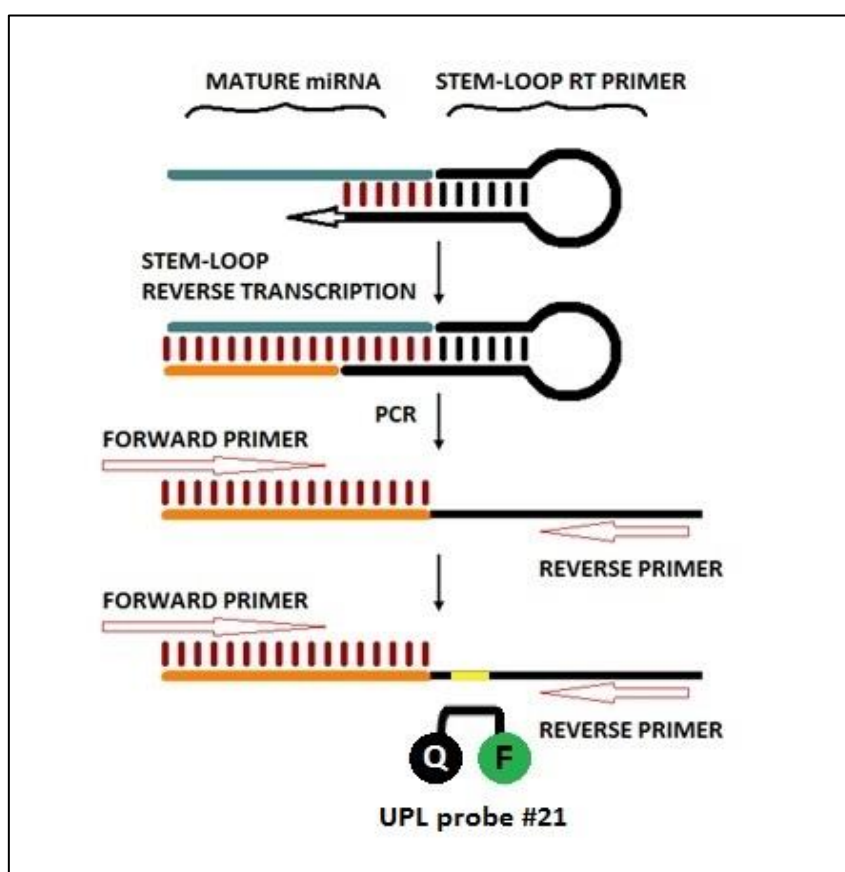
Figure 2.3 Diagrammatical representation of stem-loop RT-qPCR.
(adapted from Varkonyi-Gasic *et al*., 2007)

2.4.4 Putative miRNA target prediction

The availability of computational approaches for putative miRNA target prediction has greatly advanced the field of miRNA biology (Mendes *et al*., 2009; Mishra *et al*., 2015). Several web-based tools are available for putative miRNA target prediction. Mishra *et al*. (2015) provides a comprehensive summary of many of these methods. An extensive plant small RNA target analysis server (psRNAtarget), developed by Dai and Zhao (2011), was used in this study. This application maps miRNA sequences to the *V. vinifera* assembled transcripts based on probable miRNA/target binding capability. This calculation is based on various parameters. A maximum expectation value is assigned to score miRNA/mRNA target sequence complementarity, employing the miRU scoring system developed by Zhang (2005). psRNATarget assesses target accessibility in terms of the maximum energy (UPE) required to uncouple and expose the miRNA target site. Targets are usually chosen based on the lower UPE values of their interaction as determined by psRNATarget. The base-pairing interactions of the regions flanking the target site are also taken into account to ensure enough space is present for the RISC complex to function normally. Kertesz *et al.* (2007) suggested that 13 nucleotides downstream and 17 nucleotides upstream of the target site should be considered when assessing target accessibility.

2.4.5 miRNA-target interaction

MicroRNAs negatively regulate the expression of target genes through degradation of target mRNA (Guleria *et al*., 2011; Khraiwesh *et al*., 2012) or via transcriptional/translational repression (Guleria *et al*., 2011). This implies that the up-regulation of a miRNA would result in the down-regulation of its target gene, and vice versa. This anti-correlation forms the basis of many studies aimed at characterising plant-pathogen interactions.

Differential *V. vinifera* gene expression in response to GLRaV-3 infection has been reported in various studies on red-fruited cultivars, including Cabernet Sauvignon (Espinoza *et al*., 2007a; Espinoza *et al*., 2007b; Vega *et al*., 2011). Genes associated with berry ripening, anthocyanin biosynthesis and sugar transporters were shown to be affected, resulting in incomplete berry-ripening (Vega *et al*., 2011). Several defence- and senescence-related genes were up-regulated in GLRaV-3 infected plants (Espinoza *et al*., 2007b; Vega *et al*., 2011). Descriptions for some of these genes included receptor serine/threonine kinases, dicer-like 1, leucine-rich repeat family proteins, NAC proteins, f-box proteins and cyclin-dependent protein kinases. Induction of auxin-responsive genes, expansin and squamosa promotor-binding proteins was also reported by Espinoza *et al*. (2007a). A

recent study in our research group (Bester *et al*., 2016 unpublished data) identified several genes that were differentially expressed in response to GLRaV-3 variant group II infection, in three *V. vinifera* cultivars. Annotations for these genes included NAC transcription factors, GTPase-activating protein, glucan endo-1,3-beta-glucosidase, WAT1-related protein, expansin, thaumatin, fidgetin and lipid-transfer DIR1 protein.

Changes in grapevine miRNA levels due to viral infection has been shown in various recent reports (Alabi *et al*., 2012; Singh *et al*., 2012; Bester *et al*., 2016). Bester *et al*. (2016) validated the anti-correlation of two vvi-miRNAs (vvi-miR398b-c and vvi-miR395a-m) and their targets in Cabernet Sauvignon plants infected with GLRaV-3 variant group II. These miRNAs were predicted to target serine threonine protein kinase and ATP sulfurylase, respectively, which are important regulators in pathogen recognition, activation of plant defence mechanisms and ROS scavenging (Afzal *et al*., 2008; Zhu *et al*., 2011). Characterising these miRNA responses and validating the relationship of miRNAs and their respective targets in plant viral infection provides resources for further elucidation of compatible plant-pathogen interactions. This could also ultimately aid in the development of more targeted GLRaV-3 and GLD intervention strategies.

2.5 Conclusion

The significant impact of GLD on grape growing regions worldwide means that understanding GLRaV-3 and the interaction with its host remains a high priority. Several genetic variants of GLRaV-3 have been identified internationally, and there is growing evidence that these variants are biologically distinct. Recent studies have reported differences in transmission efficiency and prevalence of GLRaV-3 variants in vineyards around the world. Substantiating such differences in pathogenicity would provide resources for further host-pathogen interaction studies and could aid in further understanding GLRaV-3 infection and GLD etiology.

The aim of this study was to characterise *Vitis vinifera* miRNA and target expression in response to GLRaV-3 infection from different variant groups under greenhouse and field conditions.

Chapter 3: Materials and methods

3.1 Plant material

3.1.1 Greenhouse plants

All plants in this study were *Vitis vinifera* cultivar Cabernet Sauvignon. A pilot study was undertaken in 2014 to assess the use of the stem-loop RT-qPCR assay for the purpose of miRNA quantitation in grapevine. Cuttings were made from naturally-infected Cabernet Sauvignon plants and used for the establishment of twelve own-rooted plants in the Vitis laboratory greenhouse. Plants singly infected with one of four GLRaV-3 variants (I, II, III and VI) were established, with three biological replicates per variant group infection. Four healthy plant controls were obtained from a certified nursery and rooted along with the 12 infected plants under conditions of natural light, with temperatures ranging between 22 °C and 28 °C. Soil- and potting conditions included the use of five litre bags filled with a mixture of sand (45%), vermiculite (10%) and coco peat (45%). This data set will be referred to as 2014 GH.

An additional set of plants grown under greenhouse conditions was established by collecting forty-eight virus free plants from a certified nursery. These plants were planted in the Vitis laboratory greenhouse. One shoot was allowed to grow per plant, with lateral shoots being constantly removed. Plants were graft-inoculated to be singly infected with one of five genetic variants (I, II, III, VI and VII) of GLRaV-3 found in South Africa. Forty plants were grafted-inoculated, to ultimately establish a set of plants that included 8 healthy samples, and 8 biological replicates from each variant group infection. Sampling of all greenhouse plants was done in the same physiological growth stage, as soon as full cane lignification occurred. Samples were processed by removing the outer bark layers from shoots and scraping and collecting the phloem material. Phloem scrapings were stored at -80 °C. These plants were sampled twice, six months apart, to yield two data sets (2015 1 GH and 2015 2 GH) for the purpose of a time course comparison.

3.1.2 Field plants

A fourth data set (2016 field) was established by sampling plants grown under field conditions. A grapevine leafroll disease (GLD) survey of vineyards in the Stellenbosch winelands was undertaken early in 2016. Plants were sampled from vineyards that have lost their mother block status due to GLD abundance of more than 3%. These mother blocks are useful in assessing the degree of insect-

vector spread of GLRaV-3. Certified virus-free material was used for the establishment of these vineyards and as such, insect-vector spread is considered the only means of transmission of the virus. Different wine farms utilised various rootstock/scion clone combinations for the establishment of these mother blocks. An overview of all rootstock/scion combinations investigated in this study is provided in Table 3.1. Plants with classical GLD symptoms were sampled based on phenotypic assessment. Five symptomatic and five asymptomatic plants were sampled per vineyard block. Nineteen vineyards from four farms in the greater Stellenbosch region were sampled.

Table 3.1 Summary of scion and rootstock clones and rootstock cultivars of all plants.

	Vineyard block	Scion Clone	Rootstock Clone	Rootstock Cultivar
2015 Greenhouse plants				
All	N/A	CS 338 C	RQ 28 C	Richter 110
Field plants (Survey)				
Farm A	1	CS 163 I	AA 219 F	101-14
	2	CS 163 O	AA 219 F	101-14
Farm B	3	CS 34 B	AA 219 F / 662	101-14
	4	CS 169 A	AA 26 B /25 A	101-14
	5	CS 169 B	AA 219 F	101-14

3.2 RNA extraction

A CTAB buffer extraction protocol (Carra *et al*., 2007) as modified in Bester *et al*. (2014) was used for total RNA extraction from two grams of phloem scrapings. Scrapings were homogenised in liquid nitrogen and stored at -80 °C. All extracted RNA samples were split into four aliquots each and stored at -80 °C to limit the amount of RNA degradation due to repeated freeze/thaw cycles. The quality of RNA extracted for this study was assessed by spectrophotometry (Nanodrop 1000 or 2000) and gel electrophoresis (2% Tris-acetate-EDTA (TAE) agarose gel).

RNA extractions of the GLD survey were also performed using a CTAB buffer extraction protocol (Carra *et al*., 2007). To ensure enough RNA was extracted for miRNA quantitation as well as miRNA target validations, the extraction procedure was performed using the original protocol described by Carra *et al*. (2007), in which the high- and low molecular weight fractions of the total RNA sample were precipitated and stored separately. RNA samples were split into four aliquots each and stored at -80 °C to avoid repeated freeze/thaw cycles.

DNase treatment was performed using RQ1 RNase-free DNase (Promega). Five µg of total RNA were treated in 50 µl reactions, following instructions provided by the manufacturer. An acidic

phenol: chloroform-isoamyl alcohol (5:1) extraction method was used for RNA purification, followed by a 2.5x absolute ethanol and 0.1x sodium acetate (3M, pH 5.2) precipitation step. RNA pellets were washed in 70% ethanol, air-dried and resuspended in 20 µl Milli-Q H_2O. DNase-treated RNA quality was assessed by gel electrophoresis (2% TAE Agarose gel) and spectrophotometry (Nanodrop 1000 or 2000).

3.3 Virus detection

3.3.1 GLRaV-3 infection status and variant group screening

To confirm the GLRaV-3 infection status of the graft-inoculated plants in the greenhouse, initial virus screening was performed by means of a rapid one-step RT-PCR assay (MacKenzie, 1997), using primers targeting GLRaV-3 ORF1a (Bester *et al*., 2014). Screening was repeated after each round of graft inoculations. The GLRaV-3 infection status of all plant samples was confirmed using an end-point RT-PCR assay developed by Bester *et al*. (2014). A real-time PCR high-resolution melting curve RT-PCR assay (Bester *et al.,* 2012b) in combination with an end-point RT-PCR assay (Jooste *et al*., 2015) were used to verify GLRaV-3 variant status of all plants.

3.3.2 Virus concentration ratio determination

To ascertain the relative abundance of GLRaV-3 within plants, virus concentrations were normalised with three stably-expressed reference genes to produce virus concentration ratios (VCRs). Virus concentration ratios of all samples were determined using a SYBR Green RT-qPCR assay (Bester *et al*., 2014) on the Rotor-Gene Q thermal Cycler (Qiagen). Complementary DNA (cDNA) was synthesised from 1 µg of total RNA for each sample in a 20 µl reaction using 0.3 µl random hexamers (Promega), 100 U MAXIMA reverse transcriptase (Thermo Scientific) and 20 U Ribolock RNase Inhibitor (Thermo Scientific). Samples were subsequently incubated at 25 °C for 10 minutes followed by 50 °C for 30 minutes as prescribed by the manufacturer. A five-fold dilution series was prepared from pooled cDNA from each sample and used to construct a standard curve for the gene of interest (GLRaV-3 ORF1a) and three reference genes, namely Glyceraldehyde 3-phosphate dehydrogenase (GAPDH), Actin and alpha-Tubulin. The same pooled cDNA used to construct the standard curves was diluted 25X and used for the purpose of quantitation. Virus concentration ratios were quantified by comparing the expression of the ORF1a gene of GLRaV-3 to the geometric mean of the three reference genes used. All reactions were performed in triplicate in Rotor-Gene Q 0.1 ml tube-and-cap strips.

3.4 RT-qPCR miRNA expression profiling

3.4.1 MicroRNA selection and primer design

MicroRNAs investigated in this study were selected from various sources. Six miRNAs that showed significant miRNA expression differences were selected from a study by Alabi *et al*. (2012), in which differential miRNA expression between GLD and healthy samples was assessed using next-generation sequencing (NGS). Four additional miRNAs were selected based on their high expression levels in GLD samples, as determined by a previous miRNA microarray study (Bester *et al*., 2016). Two highly expressed miRNAs were selected as reference miRNAs based on their expression stability in healthy and GLD samples (Varkonyi-Gasic *et al*., 2007; Pantaleo *et al*., 2010; Alabi *et al*., 2012).

Stem-loop reverse transcription (RT) primers and specific PCR forward primers for each miRNA assayed were designed using an online tool, OligoAnalyzer (Integrated DNA Technologies) (Addendum A). The RT-qPCRs were performed using a universal reverse primer (Varkonyi-Gasic *et al*., 2007) and the Universal ProbeLibrary probe #21 (Roche Life Science) in conjunction with the miRNA-specific forward primers. All primer-design and PCR reactions were executed in accordance with the method proposed by Varkonyi-Gasic *et al*. (2007).

3.4.2 MicroRNA cDNA synthesis

Complimentary DNA (cDNA) of plants grown under greenhouse conditions was synthesised from 1 µg of total RNA in a 20 µl reaction as per manufacturer's instructions. The reaction setup consisted of 100 U MAXIMA reverse transcriptase (Thermo Scientific), 20 U Ribolock RNase Inhibitor (Thermo Scientific), 0.5 mM dNTPs (Thermo Scientific) and 1 µM stem-loop RT primer (IDT) specific to each mature miRNA. PCR cycling parameters included a 30 minute incubation step at 16 °C, followed by 60 cycles of 30 °C for 30 seconds, 42 °C for 30 seconds and 50 °C for 1 second for the purpose of 'pulsed' reverse transcription. Following the 60 cycles mentioned, samples were incubated at 85 °C for 5 minutes to deactivate enzyme activity. For cDNA synthesis from plants grown under field conditions the amount of input RNA was 500 ng. This choice was based on the higher concentration of miRNAs in the low molecular weight RNA fraction, compared to total RNA. cDNA from each sample was pooled and a five-fold dilution series prepared to construct a standard curve and a 25X dilution was used for quantitation. Single use cDNA aliquots were made for all samples and stored at -20 °C to prevent cDNA degradation from freeze/thaw cycles.

3.4.3 Probe-based RT-qPCR

MicroRNA expression levels were measured with a probe-based RT-qPCR assay (Chen *et al*., 2005; Varkonyi-Gasic *et al*., 2007) using the Rotor-Gene Q thermal cycler (Qiagen). Reaction setup included 1X Fast Start Universal Probe Master (ROX) (Roche Life Science), 0.1 µM Universal ProbeLibrary probe #21 (Roche Life Science), Milli-Q H_2O and 0.5 – 0.6 µM primers (IDT) (Addendum A.). One µl of diluted cDNA was added to each reaction to a final reaction volume of 10 µl. The five-fold dilution series constructed for each miRNA consisted of five dilution points ranging from a 5X to 3125X dilution. The 25X dilution of each sample was quantified using the miRNA-specific forward primers and universal reverse primer (Addendum A). A "no-template" control (NTC) and a "no-reverse transcription" (no-RT) control were also included in each run as control reactions. Three technical replicates of all reactions were performed in Rotor-Gene Q 0.1 ml tube-and-cap strips. Cycling conditions consisted of an activation hold of 95 °C for 10 min, followed by 45 cycles of 95 °C for 10 seconds and a 60 second annealing/extension step, in line with the protocol described by Varkonyi-Gasic *et al*. (2007). The fluorescent signal was acquired on the green channel at the end of each 60 second extension step.

3.4.4 miRNA primer specificity and quality control

Standard curve samples and controls (NTCs and no-RT) were visualised by 4% TAE agarose gel electrophoresis. Non-specific PCR products with the same size as the particular miRNA product were excised from the gel and purified using the Zymoclean™ Gel DNA Recovery Kit (Zymo Research) for cloning and sequencing. The second dilution point of miRNAs showing non-specific amplification was cloned and sequenced in parallel as a positive control. The pGEM®-T Easy Vector System (Promega) was used for cloning of amplicons according to the manufacturer's instructions. Chemically competent *Escherichia coli* JM109 cells were prepared and used for transformation purposes, following the protocol described by Sambrook *et al*. (1989). Colony PCRs were performed to confirm the presence of the correct inserts, using the T7 and SP6 vector primers. Recombinant plasmids were extracted using the GeneJET Plasmid Miniprep Kit (Thermo Scientific) and Sanger sequenced at the Stellenbosch University Central Analytical Facility (CAF), using the T7 and SP6 primers (Addendum A).

An Excel-based application, BestKeeper (Pfaffl *et al*., 2004) was used to calculate the stability of the two reference miRNAs, miR159c and miR167a, utilised in this study. The quantitation cycle (Cq) values from all samples were included in the analysis to assess expression stability.

3.5 Putative miRNA target gene expression profiling

3.5.1 Target prediction and primer design

Putative miRNA targets were predicted using a web-based application, psRNATarget (Dai and Zhao, 2011). To lower the risk of false positive predictions, the cut-off threshold of the maximum expectation value was reduced from the default value of 3.0 to 2.0. The gene ontology terms of biological processes and metabolic pathways in which these predicted targets are involved in were functionally annotated using Blast2GO (Conesa and Götz, 2008). At least one target gene for each miRNA was selected for RT-qPCR validation in two data sets (2015 2 GH and 2016 field).

Primers were designed for selected miRNA targets using a web-based PCR and qPCR primer design tool, PrimerQuest (Integrated DNA Technologies) (Addendum A). Primers were designed to span exon junctions to eliminate genomic DNA amplification. The *Vitis vinifera* annotation file was downloaded from the Grape Genome Browser of Genoscope and used to ascertain the positions of the coding sequences (CDS) for each putative miRNA target gene. Primer pairs were evaluated for target specificity using the Basic Local Alignment Search Tool (BLAST) of NCBI. A web-based application, OligoAnalyzer (Integrated DNA Technologies), was used to assess the risk of self-dimerisation and heterodimers, and also to validate the calculated melting temperatures of all primers used.

3.5.2 Target validations cDNA synthesis

Complimentary DNA was synthesised from 1 µg of total RNA or 1 µg of high molecular weight RNA for the greenhouse and GLD survey plants, respectively. The 20 µl reaction setup for cDNA synthesis included 100 U MAXIMA reverse transcriptase (Thermo Scientific), 20 U Ribolock RNase Inhibitor (Thermo Scientific) and 0.3 µl random hexamers (Promega). Samples were subsequently incubated at 25 °C for 10 minutes followed by 50 °C for 30 minutes as instructed by the manufacturer. cDNA from each sample was pooled and a five-fold dilution series prepared to construct a standard curve of the gene of interest and three reference genes, Elongation factor 1-alpha (EF1α), Ubiquitin-conjugating enzyme (UBC) and alpha-Tubulin. A 25X dilution was used for quantitation.

3.5.3 SYBR green RT-qPCR

Expression profiling of putative miRNA targets was performed using SYBR green RT-qPCR assays, utilising SensiMix SYBR® No-ROX master mix (Bioline) and the Rotor-Gene Q thermal cycler (Qiagen). The 12.5 µl reactions contained 1 X SensiMix SYBR® No-ROX master, Milli-Q H_2O and 0.4 µM forward and reverse primers (IDT) respectively (Addendum A). The pooled five-fold dilution series comprised five dilution points ranging from a 5X dilution to a 3125X dilution. The 25X dilution prepared for each sample was quantified using the specific primer pairs designed for each miRNA target gene. Requisite controls were included in all qPCR runs, which included NTC and no-RT reactions as a measure to assess the extent of genomic DNA contamination. PCR cycling parameters for all miRNA target screenings consisted of a 95 °C activation hold for 10 minutes, followed by 45 cycles of 95 °C for 15 seconds, 58 °C for 15 seconds and 72 °C for 15 seconds. An annealing step of 55 °C for 15 seconds was used for all reference genes. Acquisition on the green channel was recorded at the end of each 72 °C extension step. Each run was concluded with a melting curve analysis of all PCR amplicons in order to identify primer-dimer formation and non-specific amplification. Temperatures ranged from 65 °C to 95 °C with a 1 °C increase in temperature every 5 seconds. All reactions were performed in triplicate in Rotor-Gene Q 0.1 ml tube-and-cap strips. All PCR products were visualised by 2% TAE agarose gel electrophoresis to ensure the presence of single amplicons of the correct size for all primer pairs.

3.5.5 Reference gene stability test

An Excel-based application, BestKeeper (Pfaffl *et al*., 2004) was used to calculate the stability of the three reference genes utilised for the purpose of target validations, namely alpha-Tubulin, EF1-α and UBC. These reference genes were chosen based on their stable expression in *V. vinifera* material (Terrier *et al*., 2005; Reid *et al*., 2006). The Cq values from all samples were included in the BestKeeper analysis to assess expression stability.

3.6 Data analysis

Polymerase chain reaction efficiency, Cq values and quantitation values for all miRNAs and miRNA targets were calculated using the Rotor-gene Q software version 2.3.1 (Qiagen). This calculation is based on the slope of the standard curve generated from the pooled five-fold dilution series for each gene/miRNA. For the purpose of quantitation, all runs performed included the second dilution point (25X) of the dilution series prepared per gene/miRNA to compensate for inter-assay variability.

A web-browser application, Harbin (Bester *et al*., 2017), was recently created in our research group for the purpose of simplifying quantitative PCR data analysis. Harbin (https://rbester.shinyapps.io/Harbin/) was used for all concentration ratio (CR) calculations by comparing the expression of target genes/miRNAs to that of the references/reference gene index. The geometric means of the triplicate reactions were used for all relative quantitation calculations. The geometric mean of the concentration of the appropriate references was used for normalisation of miRNA and target expression levels. Differential expression analysis between experimental groups was performed using the Wilcoxon rank sum test. This test was selected as the most applicable considering the number of samples and data distribution. A p-value significance threshold of 0.05 was selected in all instances.

Chapter 4: Results and discussion

4.1 Plant material and RNA extraction

Plant material collected in this study was obtained from three sources and all plants were of cultivar (cv.) Cabernet Sauvignon. The 2014 GH data set consisted of 12 own-rooted cuttings of established, symptomatic infections found in commercial vineyards and rooted in the Vitis laboratory greenhouse along with four healthy controls. These plants represented variant groups I, II, III and VI. The 2015 GH data set consisted of 48 plants obtained from a certified nursery and established in the Vitis laboratory greenhouse. Forty plants were graft-inoculated in December of 2014, with the aim of establishing eight biological replicates per variant group infection (groups I, II, III, VI and VII) and eight healthy control plants. Thirty-eight plants were selected for miRNA and associated target expression profiling, including five healthy controls and seven plants from each variant group infection, except group VII, which only yielded five positive plants. The 2016 field data set was established by collecting GLD symptomatic and asymptomatic plants from commercial vineyards in the Stellenbosch region. Thirty-eight Cabernet Sauvignon plants were selected for further analyses. The virus status of these plants is discussed in more detail later.

RNA extractions using the CTAB buffer extraction protocols consistently yielded high quality RNA for RT-qPCR. This method was specifically selected for its proficiency in extracting high quality total RNA with a substantial sRNA fraction from polysaccharide-rich plant tissues. Average concentrations in ng/µl and average A260/280 and A260/230 ratios for all data sets are provided in Table 4.1.

Table 4.1 Summary of RNA extraction results across all data sets.

RNA	Average concentration* (ng/µl)	Average* A260/280	Average* A260/230
2014 GH	953.41 (330.6)	1.96 (0.04)	2.08 (0.04)
2015 1 GH	356.7 (123.9)	1.96 (0.05)	1.97 (0.08)
2015 2 GH	754.48 (341.8)	2.08 (0.06)	2.26 (0.08)
2016 field high molecular weight	564.4 (285.47)	2.09 (0.03)	2.28 (0.09)
2016 field low molecular weight	289.4 (74.67)	1.93 (0.03)	2.06 (0.09)

*Standard deviation is indicated in brackets.

On average, 55.35% high quality DNase-treated RNA was recovered following DNase treatments of 5 µg of total RNA. No RNA degradation could be detected with 2% TAE gel electrophoresis, before

or after DNase treatment. The average A260/280 and A260/230 ratios for all DNase treated RNA were 1.94 and 2.17, respectively.

4.2 Virus detection

4.2.1 GLRaV-3 infection status and variant group screening

Initial virus screening of the 2015 greenhouse plants was performed using a rapid one-step RT-PCR assay (MacKenzie, 1997) to ascertain the GLRaV-3 infection status of the newly graft-inoculated *V. vinifera* cv. Cabernet Sauvignon plants. Plants were screened at three time-points, namely 50, 77 and 105 days post-inoculation, during a two-month period. GLRaV-3 variant groups I and II graft-inoculated plants showed the most rapid infection rate, and by 50 days post-inoculation had yielded six positive plants per group, indicating that they might be transmitted more efficiently. Due to the range in transmission efficiency, not all variant group infections were represented by eight biological replicates. A minimum of five GLRaV-3 positive plants per group was deemed sufficient for comparison between variant group infections. Plants infected with variant groups VI and VII had to undergo multiple rounds of grafting to yield five positive plants per group. These findings could imply biological differences between variant groups in terms of pathogenicity. Virus concentration differences in the grafting sources could also account for the observed variability in transmission efficiency between variant group graft-inoculations. Source material with a lower VCR would likely produce grafting material with a lower abundance of that specific GLRaV-3 variant, thereby reducing the probability of virus transfer and replication in host plants.

4.2.2 Grapevine leafroll disease survey

A GLD survey was conducted early in 2016 to collect symptomatic and asymptomatic material in commercial vineyards. One hundred and seventy-five Chardonnay, Mourvedre, Shiraz, Pinot Noir and Cabernet Sauvignon symptomatic and asymptomatic plants were sampled based on phenotypic assessment, of which 113 tested positive for GLRaV-3. Symptom expression in Chardonnay and red-fruited cultivars, such as Cabernet Sauvignon, is considered more pronounced than many other cultivars, which improved the ease of visual assessment. Due to possible variability of symptom expression, five symptomatic and five asymptomatic plants were sampled per vineyard to compensate for potential false assessments. Thirty plants (26.5%) tested positive for GLRaV-3 single-variant infections, with the remaining plants showing multiple variant infections of several different combinations. The most prevalent virus variant found was GLRaV-3 variant group II in either single-

or mixed infections. The most abundant mixed infection was GLRaV-3 II/VI. These findings are in agreement with what was found by Jooste *et al*. (2015), in surveys of viruses affecting Western Cape vineyards. This study showed variant groups II and VI to be the most abundant as single-variant infections and in combination with other variants in vineyards screened. The amount of single-variant infections found in this study relative to that of Jooste *et al*. (2015) was also comparable at 26.5% and 37.8%, respectively. A summary of the GLRaV-3 variant groups present in all the vineyards sampled is provided in Figure 4.1.
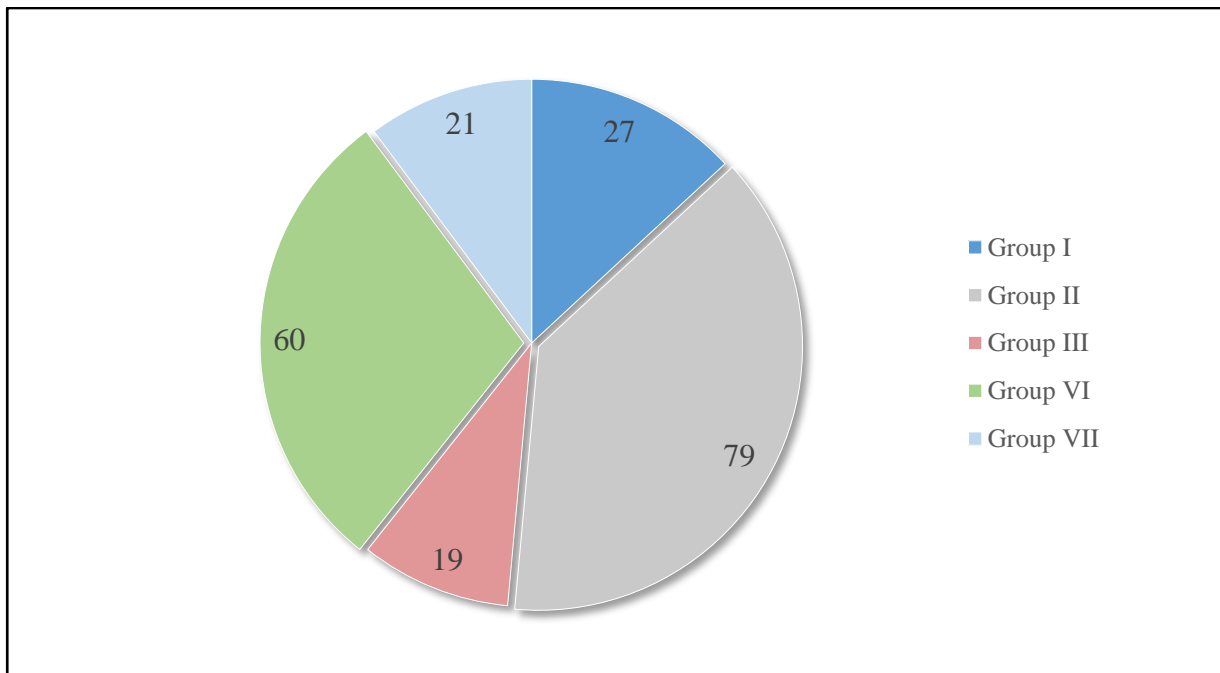
Figure 4.1 GLRaV-3 variant group presence as single and mixed infections in all survey plants screened.

For the miRNA and miRNA target expression comparisons between variant groups, only the field plants that were of the cultivar Cabernet Sauvignon were used, as this was the same cultivar that was established in the greenhouse sets. Five vineyard blocks were sampled between two farms. The trend of single-variant infections as a percentage of total infections was upheld in the Cabernet Sauvignon plants (28.6%). Thirty-eight plants, of which 23 tested positive for GLRaV-3 and 15 were negative controls, were used for RT-qPCR expression profiling of miRNAs and associated target genes. The virus-variant infection status of the GLRaV-3 positive plants is summarised in Figure 4.2. No single-variant infections for GLRaV-3 group I were found in the Cabernet Sauvignon plants sampled, confirming the low prevalence of variant group I observed in previous South African studies (Jooste *et al*., 2012; 2015). These findings are in contrast to the high prevalence of variant group I found in

other grape-growing regions around the world, including the United States of America (Napa Valley), China and New Zealand (Sharma *et al*., 2011; Farooq *et al*., 2013; Chooi *et al*., 2013a).
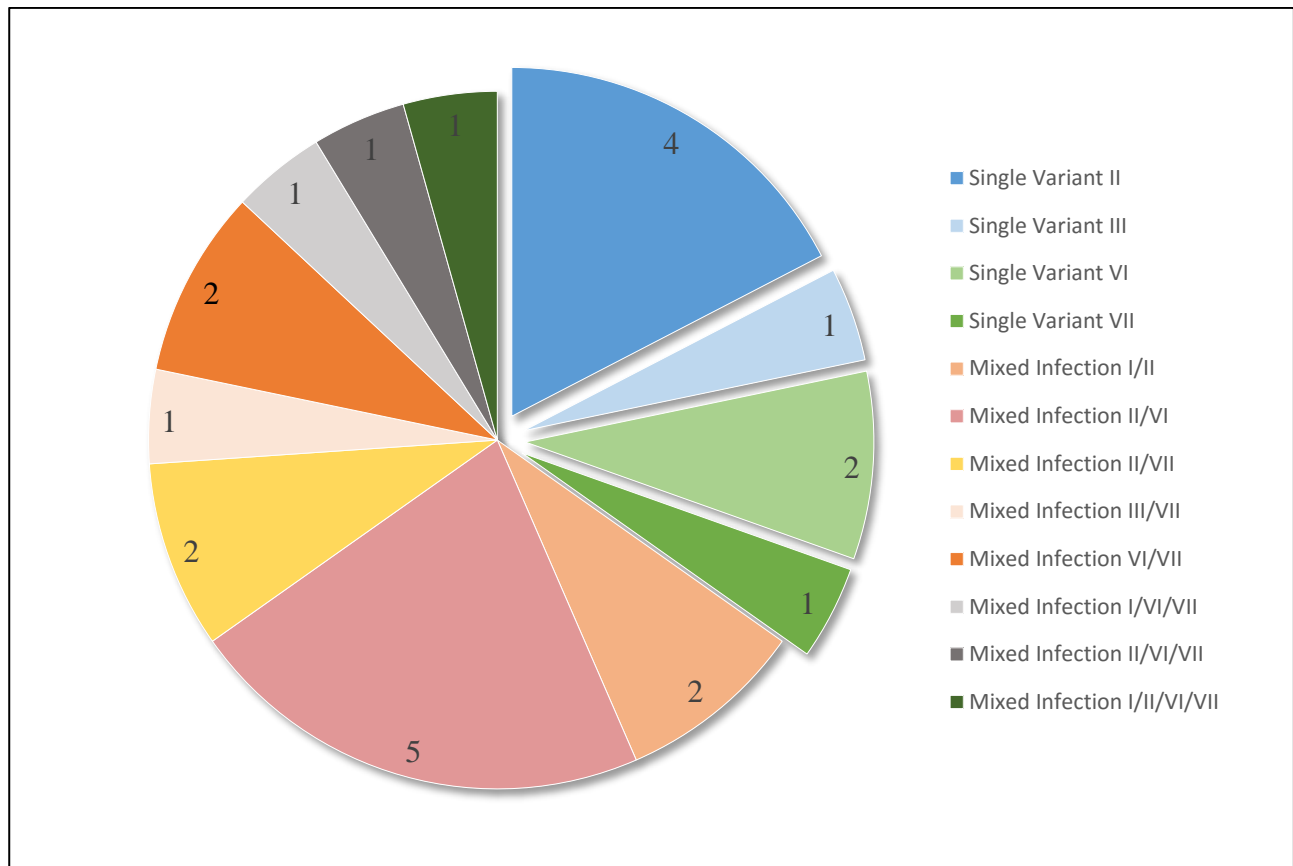
Figure 4.2 GLRaV-3 variant group infection status of all Cabernet Sauvignon plants sampled in the field. Single-variant infections are shown as elevated segments in the chart.

4.2.3 Virus concentration ratios

A SYBR Green RT-qPCR assay (Bester *et al*., 2014) with an efficiency correction was used to determine the relative concentration of GLRaV-3, expressed as virus concentration ratios (VCRs), in all samples. The three reference genes (Actin, α-Tub and GAPDH) were selected as reference gene index based on their stable expression in GLRaV-3 infected phloem material of *V. vinifera* (Bester *et al*., 2014). A summary of qPCR statistics including PCR efficiency values, correlation coefficient (r^2) values, standard curve slopes and y-intercepts is provided in Table 4.2. The PCR efficiency as calculated from all standard curves generated in this study was high and no inhibition was observed when considering the Cq values of the cDNA dilution series of each gene.

Table 4.2 RT-qPCR statistics for VCR determination of all samples.

Assay	Efficiency	r^2	Slope	y-intercept
2014 GH				
GLRaV-3 ORF1a	0.96	0.996	-3.413	27.193
actin	1.06	0.998	-3.180	25.579
GAPDH	0.97	0.995	-3.393	24.546
alpha-Tubulin	0.94	0.995	-3.469	23.998
2015 1 GH				
GLRaV-3 ORF1a	0.81	0.951	-3.893	19.595
actin	0.88	0.982	-3.645	19.694
GAPDH	0.85	0.949	-3.729	20.117
alpha-Tubulin	0.93	0.997	-3.493	23.596
2015 2 GH				
GLRaV-3 ORF1a	0.87	0.993	-3.667	17.29
actin	0.91	0.991	-3.559	18.309
GAPDH	0.72	0.99	-4.243	19.503
alpha-Tubulin	0.92	0.995	-3.524	21.153
2016 field				
GLRaV-3 ORF1a	0.93	0.996	-3.488	19.609
actin	0.91	0.990	-3.568	19.590
GAPDH	0.93	0.997	-3.505	19.297
alpha-Tubulin	0.95	0.999	-3.459	22.059

4.2.3.1 Virus concentration ratios per data set

A summary of the mean VCRs of all samples in each data set is provided in Figure 4.3. The 2016 field data set showed the highest average VCR (1,37) calculated for all GLRaV-3 positive plants. The 2015 2 GH data set had the lowest average VCR (1,05) of the four data sets. No statistically significant differences in mean VCRs were observed between data sets. This finding is of interest when considering the substantial differences between plants comprising these data sets. Plants differed in terms of origin, duration of infection, rootstock, growing conditions and the number of GLRaV-3 variants co-infecting the same plant (Figure 4.2). For plants sampled as part of the GLD survey, possible co-infection with other frequently-occurring grapevine viruses could also influence VCR results, although these viruses were not specifically tested for. The lack of statistically significant differences in mean VCRs between data sets, despite likely differences in the duration of GLRaV-3 infection between these plants is intriguing. This finding suggests that the detrimental effect of GLRaV-3 over time is not directly proportional to the abundance of the virus within the host plant.
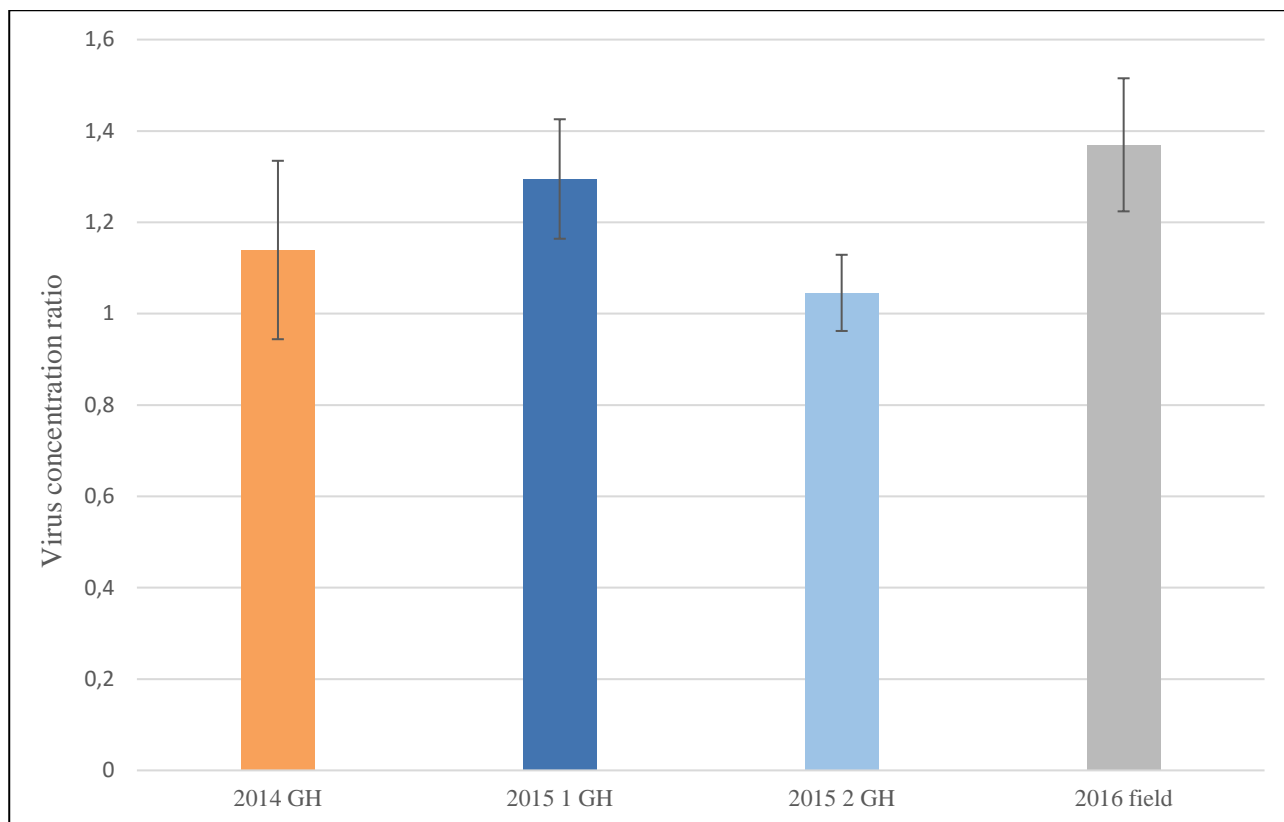
Figure 4.3 Mean virus concentration ratios across all GLRaV-3 variant group infections calculated for each data set. Bars indicate standard error.

4.2.3.2 Virus concentration ratios per variant group in greenhouse plants

Comparisons were made between VCRs calculated for plants singly infected with different variants of GLRaV-3 to identify possible biological distinctions between variants. Variant groups I and II showed consistently higher VCRs when compared to groups III, VI and VII (Figure 4.4). This trend was upheld in all greenhouse data sets, possibly indicating variability in the efficiency of virus replication within host grapevine plants between GLRaV-3 variants. Statistically significant differences in VCRs were observed in five instances (Table 4.3).

Table 4.3 Summary of VCR comparison between variant groups of GLRaV-3 in the greenhouse data sets.

	2014 GH		2015 1 GH		2015 2 GH	
	p-value	log$_2$ (fold change)[a]	p-value	log$_2$ (fold change)	p-value	log$_2$ (fold change)
Group I vs II	0.7	0,2278264	0.06494	-0,5669464	0.4634	0,3073683
Group I vs III	0.1	-1,137243	0.01515 *	-0,7816216	0.2593	-0,361043
Group I vs VI	0.1	-1,81377	0.009524 *	-1,620869	0.01748 *	-0,7092419
Group I vs VII	--	--	0.02381 *	-1,305722	0.7551	-0,3391403
Group II vs III	0.1	-1,365069	0.8182	-0,2146753	0.07211	-0,6684113
Group II vs VI	0.1	-2,041597	0.06667	-1,053923	0.01399 *	-1,01661
Group II vs VII	--	--	0.09524	-0,7387756	0.09324	-0,6465086
Group III vs VI	0.1	-0,6765274	0.1143	-0,8392476	0.8048	-0,3481989
Group III vs VII	--	--	0.1667	-0,5241003	0.7551	0,02190273
Group VI vs VII	--	--	0.8571	0,3151473	0.1061	0,3701016

* Statistically significant differences as determined with the Wilcoxon rank sum test. A p-value significance threshold of 0.05 was selected.
[a] The log$_2$ (fold change) values indicate the expression of the last variant group mentioned per line versus the first group. (i.e. last group/first group).

The VCRs of plants infected with GLRaV-3 variant group I and II were significantly higher when compared to variant groups VI and VII in both 2015 GH data sets. The 2014 GH data set yielded no statistically significant VCR differences between variant groups. This was due to the limited number of biological replicates (three) compared per variant group. Comparisons with variant group VII was also not possible for the 2014 GH data set, as it only consisted of variant groups I, II, III and VI.
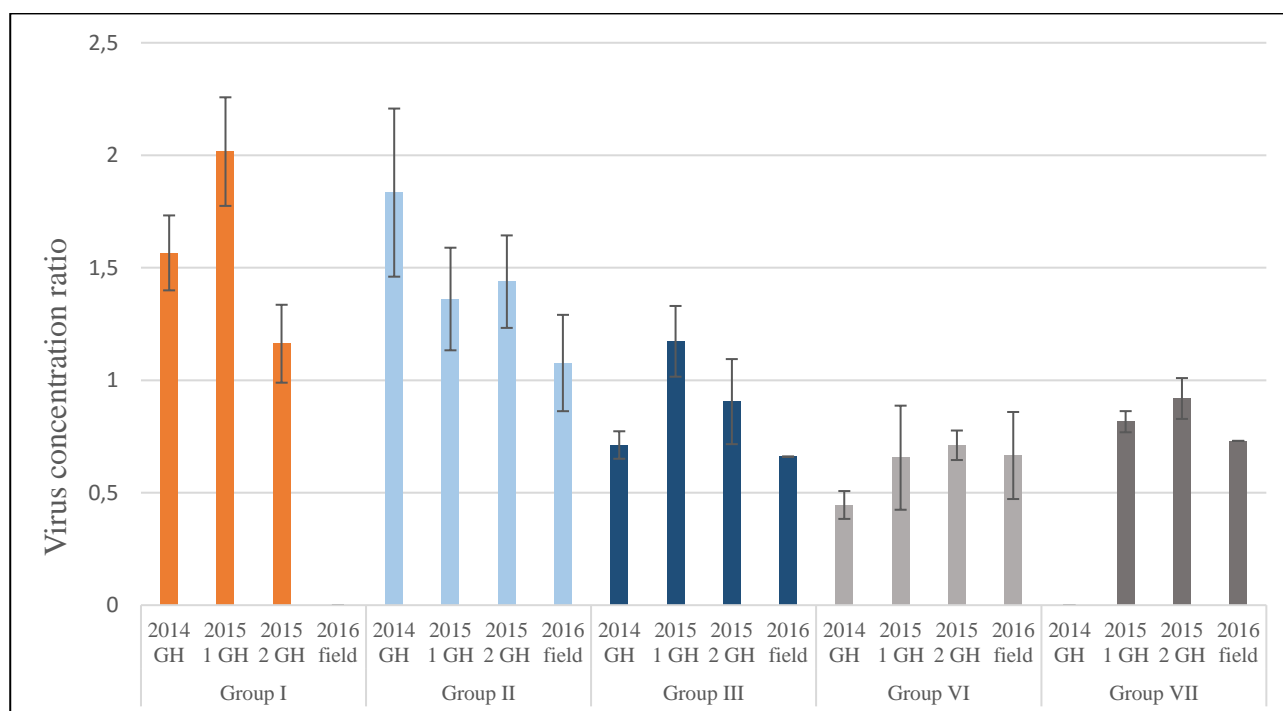
Figure 4.4 Mean virus concentration ratios calculated for each GLRaV-3 variant group infection in the four data sets. Bars indicate standard error.

31

4.2.3.3 Virus concentration ratios of field plants

A statistically significant difference (p=0.0007669) in VCRs was calculated for plants showing single-variant infections relative to plants infected with multiple GLRaV-3 variants. The VCRs of single-variant infected plants were significantly lower [$\log_2$ (fold change) value of -0.8947] compared to multiple-variant infected plants. This finding suggests that the GLRaV-3 variants did not have a competitive effect on the proliferation of the other variant groups present in the same plant. This could also be an indication that two or more virus variants act in synergy by co-expressing suppressors of silencing for example. This is indicated by the higher average VCR calculated for plants showing multiple variant infections. No statistically significant differences in VCRs were measured between plants from the two different farms sampled for the 2016 field data set. The comparison of VCRs between single-variant infected field plants was complicated due to the limited number of plants per variant group infection (Figure 4.1).

4.3 RT-qPCR miRNA expression profiling

4.3.1 Primer efficiency and specificity

The primer sets used for miRNA quantitation had an efficiency mean value of 0.86 across all miRNAs in all four data sets. No evidence of inhibition was observed when considering the Cq values of dilution series prepared for each miRNA. The linearity and reproducibility of the assay across all miRNAs was shown to be high, as indicated by an average r^2 value of 0.99. The specificity of primer pairs was confirmed by means of 4% TAE gel electrophoresis. Table 4.4 shows all PCR efficiencies, r^2 values, standard curve slopes and y-intercepts generated during miRNA expression profiling using RT-qPCR.

Table 4.4 RT-qPCR statistics for miRNA expression profiling.

Assay	Efficiency	r^2	Slope (-)	y-intercept		Efficiency	r^2	Slope (-)	y-intercept
		2014 GH					2015 1 GH		
miR159c	0.95	0.982	3.435	23.206	miR159c	0.81	0.981	3.885	21.675
miR167a	1.00	0.996	3.332	25.933	miR167a	0.8	0.992	3.899	20.213
miR408	0.79	0.993	3.959	18.79	miR408	0.8	0.99	3.933	19.889
miR399e	1.00	0.99	3.325	26.919	miR399e	0.93	0.992	3.513	26.299
miR398b	0.7	0.978	4.362	21.731	miR398b	0.81	0.99	3.885	19.638
miR397a	0.88	0.992	3.657	23.635	miR397a	0.63	0.991	4.727	21.695
miR393a	0.98	0.996	3.372	31.449	miR393a	0.65	0.99	4.61	28.675

Table 4.4 Continued from previous page.

Assay	Efficiency	r^2	Slope (-)	y-intercept		Efficiency	r^2	Slope (-)	y-intercept
miR166h	0.86	0.99	3.715	21.337	miR166h	0.75	0.978	4.128	19.384
miR164a	0.92	0.997	3.525	19.296	miR164a	0.7	0.981	4.318	18.071
miR162	0.86	0.991	3.711	23.687	miR162	0.91	0.99	3.567	16.502
miR156g	1.00	0.988	3.324	28.919	miR156g	0.72	0.99	4.238	24.874
		2015 2 GH					2016 field		
miR159c	1.05	0.983	3.197	20.964	miR159c	0.9	0.985	3.587	19.553
miR167a	0.94	0.988	3.484	25.087	miR167a	0.9	0.993	3.598	19.912
miR408	0.96	0.99	3.421	24.076	miR408	0.8	0.989	3.911	26.755
miR399e	0.71	0.99	4.427	30.849	miR399e*	--	--	--	--
miR398b	0.95	0.988	3.456	24.222	miR398b	0.81	0.995	3.894	25.795
miR397a	1.00	0.992	3.311	25.947	miR397a	0.78	0.99	3.997	27.322
miR393a	0.98	0.992	3.375	30.665	miR393a	0.84	0.991	3.787	26.695
miR166h	0.7	0.982	4.363	21.363	miR166h	0.9	0.993	3.601	19.352
miR164a	0.99	0.994	3.358	22.312	miR164a	0.88	0.995	3.639	20.795
miR162	0.92	0.996	3.518	22.555	miR162	0.81	0.986	3.892	20.799
miR156g	0.99	0.988	3.352	29.06	miR156g	0.84	0.989	3.765	29.23

*This miRNA showed the least potential for being differentially expressed in the greenhouse data sets, and as such was not included for validation in the field plants.

The stability of the two reference miRNAs, miR159c and miR167a, was assessed using an Excel-based application, BestKeeper (Pfaffl *et al.*, 2004). Descriptive statistics and pair-wise correlation analyses were performed to ensure the credibility of using these reference miRNAs for normalisation of target miRNA expression levels. BestKeeper results showed that both miRNAs were stably expressed in grapevine phloem tissue in all data sets. The average standard deviation in Cq values for miR159c and miR167a was 0.46 and 0.45, respectively. Both miR159c and miR167a had high average correlation coefficients (0.7925 and 0.7927) and power (x-fold) values (1.91 and 1.98).

4.3.2 MicroRNA expression

The concentrations of nine *V. vinifera* miRNAs were normalised with the two reference miRNAs to produce concentration ratios (CRs), using a probe-based stem-loop RT-qPCR assay (Chen *et al.*, 2005; Varkonyi-Gasic *et al.*, 2007). Several miRNAs showed statistically significant expression modulation between GLRaV-3 infected and healthy samples in the different data sets. These results are summarised in Table 4.5.

Table 4.5 Differentially expressed miRNAs across all data sets.

Data set	$\log_2$ (fold change)[a]	p-value
2014 GH		
miR408	2.830734	0.01319
miR398b	2.393181	0.01978
miR397a	1.376623	0.05824*
miR164a	-0.5376954	0.02967
miR162	-0.3850385	0.02967
2015 1 GH		
miR397a	-0.9089252	0.01909
miR162	-0.7476287	0.0312
2015 2 GH		
miR166h	-0.746873	0.007346
2016 field		
miR408	-0.9884125	0.005518
miR398b	-1.5173534	0.0001185
miR397a	-1.733065	1.461E-06

*This value is above the p-value threshold of 0.05; however, the significant $\log_2$ (fold change) value warrants inclusion of this miRNA.

[a]$\log_2$ (fold change) was calculated as diseased/healthy.

4.3.2.1 MicroRNA expression per data set

Five miRNAs were significantly modulated in GLRaV-3 infected plants of the 2014 GH data set (Table 4.5). Three miRNAs (miR398b, miR408 and miR397a) showed significant up-regulation, whereas miR164a and miR162 were down-regulated in diseased plants. The higher abundance of miR397a in infected grapevine in this data set is in contrast to what was observed in the other data sets of this study, as will be discussed later. The up-regulation of miR398b and miR408 in the GLRaV-3 infected plants of the 2014 GH data set is consistent with reports recently produced in our research group (Bester *et al*., 2016). miR398b has been studied extensively for its role in plant stress responses, including biotic stress (Zhu *et al*., 2011). miR398b was predicted to target serine threonine-protein kinases which are key regulators in plant growth and development, signalling, activation of plant defence mechanisms and scavenging of reactive oxygen species in *Arabidopsis thaliana* (Afzal *et al*., 2008; Zhu *et al*., 2011). The miR398 family is highly conserved in higher plants and as such is likely to also have conserved functions in other plants (Zhang *et al*., 2006, 2008; Sunkar and Jagadeeswaran 2008). Down-regulation of miR162 in GLD symptomatic grapevine was also reported by Alabi *et al*. (2012), whereas the lower levels of miR164a GLRaV-3 infected grapevine observed in this study was not consistent across both studies. The higher abundance of miR164a is consistent with reports by Bazzini *et al*. (2009) who showed a virus-induced increase in the levels of miR164 and its target gene in *A. thaliana*.

34

The 2015 1 GH data set showed statistically significant expression modulation in only two miRNAs, miR397a and miR162. An additional miRNA (miR408), though not statistically significant, showed notable up-regulation in GLRaV-3 infected plants in this data set, with a $\log_2$ (fold change) value of 0.915. The relative up-regulation of miR408 was consistent between the 2014 GH and 2015 1 GH data sets. Bester *et al*. (2016) reported significant up-regulation of vvi-miR408, and its known plant homologue cca-miR408, in GLRaV-3 infected grapevine using sRNA NGS, microarray data and stem-loop RT-qPCR validation. miR162 was significantly down-regulated in both the 2014 GH and 2015 1 GH data sets and was predicted to target disease resistance proteins implicated in the plant defence response. The down-regulation of miR162 could suggest a possible increase in its target genes, thereby contributing to the plant's disease resistance response. The down regulation of miR397a in GLRaV-3 infected plants was observed in three of the four data sets (2015 1 GH, 2015 2 GH and 2016 field). This down-regulation is in agreement with a report by Singh *et al*. (2012), who showed suppression of the miR397 family in virus-infected grapevine. The consistent modulation of miR397a in this study could serve as an indication that this miRNA may play an important role in the plant response to GLRaV-3 infection. The predicted targets of miR397a are laccase enzymes (Addendum B) which are involved in various processes including oxidation-reduction, lignin catabolism and copper ion binding. These enzymes are located in the apoplast, which is the primary site of contact with invasive pathogens and essential to the signalling of defence responses to biotic stressors (Bolwell *et al*., 2001; Sgherri *et al*., 2013).

The only miRNA that showed statistically significant differential expression in the 2015 2 GH data set was miR166h, although miR397a and miR156g also showed notable down-regulation in the diseased state, with $\log_2$ (fold change) values of -0.6449 and -0.791, respectively. Down-regulation of miR166h in this data set is in contrast to what was found by Alabi *et al*. (2012), who showed significant up-regulation of miR166h in GLD positive leaves of own-rooted Merlot plants. The difference in tissue type and grapevine cultivar could likely contribute to differences observed in the expression of miR166h between these two studies. The lower abundance of miR156g in GLD symptomatic vines found in this study is in agreement with what was found by Alabi *et al*. (2012). Members of the miR156 family have been shown to target squamosa promotor-binding-protein-like (SPL) transcription factors (Wang *et al*., 2011b). These transcription factors affect a wide range of plant developmental processes, including anthocyanin accumulation, leaf size and initiation rate (Gou *et al*., 2011; Wang *et al*., 2011b).

Three miRNAs (miR408, miR398b and miR397a) were differentially expressed in the 2016 field data set. These miRNAs showed significant down-regulation in GLRaV-3 infected plants. Several recent reports on miRNA expression in plant stress have also shown a congruent down-regulation of miR408, miR398b and miR397a, as studied in *V. vinifera* and *A. thaliana* (Sunkar 2010; Zeng *et al.*, 2010; Zhang *et al.*, 2011; Singh *et al.*, 2012).

4.3.2.2 Comparison of miRNA expression between data sets

The miRNA expression of plants from the different data sets varied considerably. There were several distinctions to be made between the properties of the plants utilised in each data set. Plants differed in terms of growing conditions, rootstock, age and duration of infection.

The 2014 GH data set showed the highest number (five) of differentially expressed miRNAs between diseased and healthy samples. The 2015 1 GH and 2015 2 GH data sets yielded limited statistically significant results. Both the 2014 GH and 2015 GH data sets are of the same cultivar, grown under the same greenhouse conditions. The main differences between these plants is that the 2014 GH data set consists of own-rooted plants established before the 2015 GH data sets, which are plants that were grafted onto rootstocks (Table 3.1) and established at the end of 2014. The lower degree of significant miRNA expression modulation seen in grafted Cabernet Sauvignon plants relative to own-rooted plants is consistent with results recently obtained in our research group (Bester *et al.*, 2016 unpublished data). In this study, next-generation sequencing was used to profile the sRNA response of different *V. vinifera* cultivars to infection with GLRaV-3 variant group II. The grafted Cabernet Sauvignon plants yielded no differentially expressed miRNAs, whereas 12 differentially expressed miRNAs were validated in the own-rooted Cabernet Sauvignon plants. It was hypothesised that the difference in miRNA response to GLRaV-3 infection could be a result of a more established infection in the own-rooted plants. The own-rooted plants were established before the grafted plants and are the same variant group II infected plants used in the 2014 GH data set in this study.

Differential miRNA expression in the 2016 field data set was also more pronounced than the 2015 GH data sets. The 2015 GH and 2016 field sets all consist of plants that were grafted onto different rootstocks (Table 3.1). Apart from growing conditions differing between the greenhouse and field plants, these data sets differed substantially in terms of age. Vineyards from the 2016 field data set were established in 2003 and 2011, and written off in 2011 and 2015 (farms B and A, respectively). Therefore, the GLRaV-3 infection in these plants could be more established compared to the 2015

GH data sets. The data suggests an association between miRNA expression in GLRaV-3 infection and the age of the plant/duration of infection.

4.3.2.3 MicroRNA expression between single-variant infections in greenhouse plants

The availability of single-variant infected plants allowed for comparisons to be made which could shed light on possible differences in the host-pathogen interactions of GLRaV-3 variants. The effect of multiple-variant infections on miRNA expression could also be assessed in the 2016 field data set.

MicroRNA expression patterns of different GLRaV-3 variant group infections varied substantially for several miRNAs. In many instances the direction of miRNA expression regulation between GLRaV-3 variant group infections was not the same, as some variant groups would show up-regulation and some groups were shown to be down-regulated for the same miRNA. This was evident when comparing miRNA CRs of each variant group infection to healthy plants for each miRNA. One miRNA (miR393a) showed this variable trend of regulation across all three greenhouse data sets. A recent report by Zhang *et al*. (2011) showed the modulation of the miR393 family in *Arabidopsis* leaves subjected to biotic stress, while Alabi *et al*. (2012) reported a down-regulation of this miRNA family in GLD symptomatic grapevine leaves. The inconsistent directionality of miRNA regulation between variant group infections observed in this study contributed to the lack of statistically significant measurement of expression modulation when comparing all diseased and healthy plants per miRNA. Three additional miRNAs (miR398b, miR166h and miR164a) showed this trend in two of the three greenhouse data sets. The lack of consistency in the directionality of miRNA regulation of the same miRNA between data sets, and between GLRaV-3 variant infections highlights the complexity of miRNA regulation in GLRaV-3 infection. This varying pattern of regulation between variant group infections for the same miRNA could suggest a more variant-specific response to infection for these miRNAs.

The 2014 GH data set yielded no statistically significant expression differences when comparing individual groups to healthy samples or to other variant group infections. This was due to the limited number of biological replicates (three) compared per variant group. Three miRNAs (miR408, miR397a and miR156g) in the 2015 1 GH data set showed statistically significant differential expression in individual variant group infections compared to healthy plants. In two of these instances (miR397a and miR156g) it was variant group I that was differentially expressed, and it is also the variant group that showed the highest calculated VCRs for this data set (Figure 4.4). The 2015 2 GH data yielded only one miRNA (miR166h) that showed differential expression for specific virus

variants groups (II and VII) compared to healthy plants. Plants from variant group II had the highest mean VCR for this data set (Figure 4.4). These findings could indicate a correlation between VCR and miRNA expression in GLRaV-3 infection.

For variant groups I, II, III and VI the degree of regulation was mostly proportional to the VCR determined for that specific variant group infection, i.e. the variant group infections with higher calculated VCRs showed greater $\log_2$ (fold change) values. This was not always seen for GLRaV-3 variant group VII infections. These plants had the second lowest average VCRs across all data sets yet often had the greatest miRNA $\log_2$ (fold change) values compared to healthy plants. miRNA expression in variant group VII infected plants also showed the highest degree of differential regulation relative to other variant group infections (mostly groups I and II). This finding is of interest when considering that GLRaV-3 group VII shares only 63 to 65% sequence similarity with the other variants in this study (Maree *et al*., 2015). The fact that group VII is the most divergent variant investigated, combined with the marked differences in miRNA expression and lower VCRs observed for these plants could indicate a more effective plant response to infection with this virus variant. Establishing exactly how these variants differ on a molecular level, and how the sequence variation between virus variants affect viral gene regulation could facilitate our understanding of plant-pathogen interactions in GLRaV-3 infection.

4.3.2.4 MicroRNA expression in field plants

The differential miRNAs in the 2016 field data set, miR408, miR398b and miR397a showed similar expression trends between diseased and healthy samples across the two farms. In all three cases the down-regulation observed for the specific miRNAs was the most pronounced for plants sampled from farm B. A summary of mean concentration ratios of these three miRNAs between the different vineyard blocks sampled is provided in Figure 4.5. No statistically significant differences in miRNA CRs were measured between single- and multiple-variant group infected plants in the 2016 field data set. Both farms utilised the same rootstock for all plants sampled (101-14), however, the scion clones used in the five vineyards differed (Table 3.1). Given the prominent differences in miRNA regulation observed between the two farms, it was of interest to investigate what distinctions could be made between plants from these farms. Farm A utilised the same scion/rootstock clone combination for both vineyard blocks, whereas farm B used several different combinations (Table 3.1). The three scion clones, CS 163, CS 34 and CS 169 differed in terms of where the original donor plant was obtained. The original plant for CS 163 was found in Germany (1988), whereas CS 34 and CS 169 clones originated from plants established in Davis, California (1992) and France (1988), respectively.

The most apparent difference between the vineyards from the two farms is the time at which they were established. The vineyards from farm B were established in 2003, several years before the establishment of the vineyards in farm A (2011). Vineyard blocks from farm B had already lost their mother block status, due to a GLD presence of more than 3%, by the time the vineyard blocks from farm A were first established (2011). The infection status of plants from farm B is therefore likely more established than that of farm A. This finding correlates with what was found in the greenhouse data sets, and data recently generated in our research group by Bester *et al*. (2016 unpublished). These trends suggest a greater miRNA response in plants having a longer and more established infection of GLRaV-3, and not necessarily correlated with virus concentration.
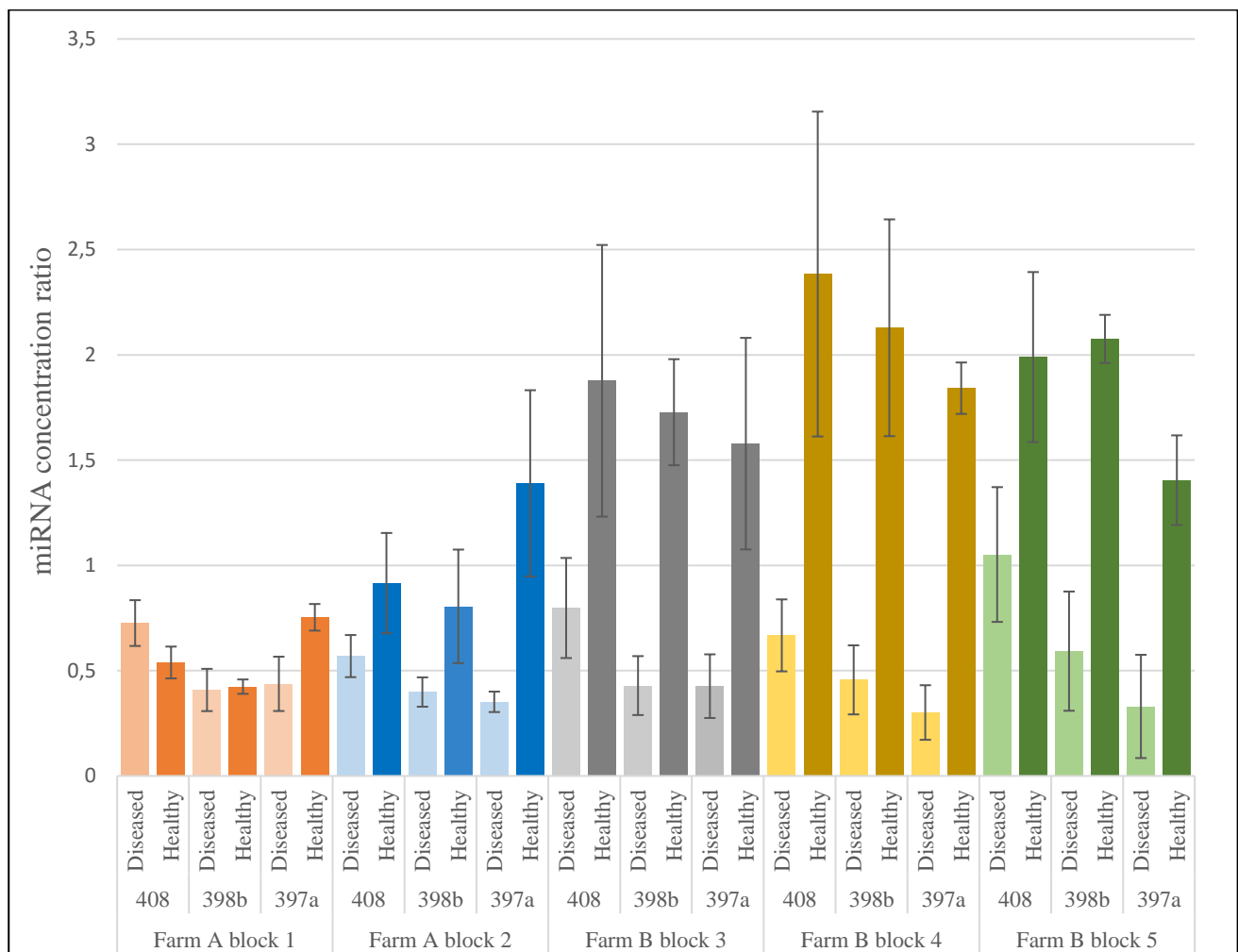
Figure 4.5 Comparison of miRNA concentration of miR408, miR398b and miR397a per vineyard sampled in the 2016 field data set. Vineyard blocks are colour-labelled, ranging from orange to green. Bars indicate standard error.

4.4 RT-qPCR target gene expression profiling

4.4.1 Target prediction and selection

Putative miRNA target prediction with psRNAtarget (Dai and Zao, 2011) and annotation using Blast2GO (Conesa and Götz, 2008) yielded several candidate genes for validation with RT-qPCR. The predicted targets for the miRNAs investigated are genes involved in growth and developmental processes, disease resistance, apoplastic processes, oxidation-reduction processes, lignin catabolism and regulation of transcription. At least one miRNA target gene was assayed for each miRNA investigated. Eleven target genes (Table 4.6) were selected based on the probability of miRNA/target interaction, as assessed using psRNAtarget. The expression of the selected miRNA targets was validated in the 2015 2 GH and 2016 field data sets using RT-qPCR.

Table 4.6 Putative miRNA targets selected for RT-qPCR validation.

	Target accession	Target description	GO annotation*
miR408_target	GSVIVT01018246001	rRNA processing isoform 1	C:nucleus
miR399e_target	GSVIVT01021449001	PREDICTED: uncharacterised protein LOC100265752	--
miR398b_target	GSVIVT01000937001	serine threonine-protein kinase pbs1	C:plasma membrane; F:protein serine/threonine kinase activity; F:non-membrane spanning protein tyrosine kinase activity; F:ATP binding; P:pattern recognition receptor signalling pathway; P:defence response to bacterium, incompatible interaction; P:peptidyl-tyrosine phosphorylation; P:protein autophosphorylation
miR397a_target	GSVIVT01034003001	laccase-4-like	C:apoplast; F:copper ion binding; F:hydroquinone:oxygen oxidoreductase activity; P:glucuronoxylan metabolic process; P:xylan biosynthetic process; P:lignin catabolic process; P:oxidation-reduction process
miR393a_target 1	GSVIVT01010995001	Protein transport inhibitor response	C:SCF ubiquitin ligase complex; F:inositol hexakisphosphate binding; F:ubiquitin-protein transferase activity; F:auxin binding; F:auxin receptor activity; P:ubiquitin-dependent protein catabolic process; P:auxin-activated signalling pathway; P:stomatal complex morphogenesis; P:pollen maturation; P:lateral root formation; P:protein ubiquitination; P:regulation of circadian rhythm; P:stamen development
miR393a_target 2	GSVIVT01033011001	Protein auxin signalling f-box 2-like	F:inositol hexakisphosphate binding; P:auxin-activated signalling pathway

40

Table 4.6 Continued from previous page.

	Target accession	Target description	GO annotation*
miR166h_target	GSVIVT01035612001	Homeobox leucine zipper ATHB-15	C:nucleus; F:DNA binding; P:positive regulation of cell proliferation; P: primary shoot apical meristem specification; F:lipid binding; P:positive regulation of cell differentiation; P:xylem development
miR164a_target	GSVIVT01007982001	nac domain-containing protein 100	C:nucleus; F:DNA binding; P:transcription, DNA-templated; P:regulation of transcription, DNA-templated
miR162_target	GSVIVT01027276001	Disease resistance rpp13-like protein 1	F:ADP binding
miR156g_target 1	GSVIVT01033519001	Squamosa Promotor-binding-like protein 9	C:nucleus; F:DNA binding
miR156g_target 2	GSVIVT01010522001	Squamosa Promotor-binding-like protein 16	C:nucleus; F:DNA binding

*GO annotations if available: C=Cellular component, F=Molecular function, P=Biological process.

4.4.2 Primer efficiency and specificity

The designed primer pairs yielded a high degree of linearity and reproducibility across all miRNA targets screened in the two data sets, 2015 2 GH and 2016 field, with mean efficiency and r^2 values of 0.95 and 0.99, respectively. A summary of all PCR efficiencies, r^2 values, standard curve slopes and y-intercepts for miRNA target expression profiling is shown in Table 4.7. No evidence of inhibition was found when considering Cq values of dilution series prepared for each gene. The specificity of all assays was validated by 2% TAE gel electrophoresis.

Table 4.7 qPCR statistics for miRNA target gene expression profiling.

Assay	Efficiency	r^2	Slope	y-intercept
2015 2 GH				
α-Tub (Ref)	0.95	0.992	-3.453	23.315
EF1-α (Ref)	1.04	0.999	-3.236	25.348
UBC (Ref)	0.94	0.994	-3.483	21.869
miR408_target	0.90	0.991	-3.598	26.716
miR399e_target	0.90	0.993	-3.588	24.709
miR398b_target	1.06	0.992	-3.186	25.656
miR397a_target	1.00	0.997	-3.317	24.874
miR393a_target 1	1.00	0.993	-3.331	21.761
miR393a_target 2	0.92	0.994	-3.542	22.151
miR166h_target	1.01	0.996	-3.308	24.458

Table 4.7 Continued from previous page.

Assay	Efficiency	r^2	Slope	y-intercept
2015 2 GH				
miR164_target	0.92	0.986	-3.544	26.407
miR162_target	0.98	0.997	-3.381	24.190
miR156g_target 1	0.93	0.985	-3.492	25.343
miR156g_target 2	0.93	0.983	-3.511	26.178
2016 field				
α-Tub (Ref)	0.95	0.999	-3.459	22.059
EF1-α (Ref)	0.94	0.991	-3.482	24.718
UBC (Ref)	0.90	0.997	-3.601	22.449
miR408_target	1.08	0.990	-3.135	25.973
miR399e_target *	--	--	--	--
miR398b_target	0.85	0.993	-3.759	24.065
miR397a_target [a]	--	--	--	--
miR393a_target 1	0.94	0.995	-3.472	24.122
miR393a_target 2	0.90	0.998	-3.592	22.733
miR166h_target	0.93	0.993	-3.508	23.162
miR164_target	0.84	0.991	-3.779	24.326
miR162_target	0.90	0.995	-3.592	21.993
miR156g_target 1	1.03	0.990	-3.254	28.427
miR156g_target 2	0.93	0.980	-3.492	21.268

*miR399e was not assayed in the 2016 field data set due to a lack of significant expression trends in greenhouse trials for this miRNA. [a] RT-qPCR for miR397a_target failed.

BestKeeper (Pfaffl *et al*., 2004) was used to calculate the stability of the three reference genes utilised, namely EF1-α, α-Tubulin and UBC. Descriptive statistics and pair-wise correlation analyses were performed to ensure the credibility of using these reference genes for normalisation of target gene expression levels. These genes were chosen for their comparable expression levels relative to that of the target genes, based on the quantitation cycle (Cq) values of the pooled samples. A Cq range of 5 was chosen as sufficient for this purpose. BestKeeper results showed a high expression stability for the three reference genes in both data sets. The average standard deviation in Cq values for EF1-α, α-Tubulin and UBC were 0.455, 0.625 and 0.325, respectively. EF1-α, α-Tubulin and UBC had high average correlation coefficients (0.895, 0.889 and 0.772, respectively) and power (x-fold) values (1.91, 2.37 and 1.66, respectively). All three reference genes could be used for normalisation.

4.4.4 Target gene expression

The concentrations of the miRNA target genes were normalised with a reference gene index comprising the three stably expressed reference genes (EF1-α, α-Tub and UBC). Seven putative miRNA targets showed statistically significant expression modulation between diseased and healthy

samples. Four miRNA target genes were differentially expressed in the 2016 field data set, compared to the three differential target genes validated in the 2015 2 GH data set (Table 4.8).

Table 4.8 Putative miRNA targets showing statistically significant expression modulation between diseased and healthy samples.

Data set	log$_2$ (fold change)[a]	p-value	psRNAtarget	Target description
2015 2 GH				
miR393a_target 2	0.40984444	0.02535	GSVIVT01033011001	Protein auxin signalling f-box 2-like
miR156g_target 1	-0.88645276	0.0156	GSVIVT01033519001	Squamosa Promotor-binding-like protein 9
miR156g_target 2	-0.89153191	0.01305	GSVIVT01010522001	Squamosa Promotor-binding-like protein 16
2016 field				
miR408_target	-0.620384	0.02378	GSVIVT01018246001	rRNA processing isoform 1
miR166h_target	-0.2860509	0.00092	GSVIVT01035612001	Homeobox leucine zipper ATHB-15
miR162_target	-0.5860558	0.04124	GSVIVT01027276001	Disease resistance rpp13-like protein 1
miR393a_target 1	-0.1743746	0.02013	GSVIVT01010995001	Protein transport inhibitor response

[a]log$_2$ (fold change) was calculated as diseased/healthy.

Of the seven differentially expressed miRNA target genes, only one gene (miR393a_target 2) showed a significant up-regulation in GLRaV-3 infected samples. Expression modulation of the miR393 family has been reported in various studies on plant biotic stress response (Navarro *et al*., 2006; Ruiz-Ferrer and Voinnet, 2009). These target genes are involved in protein transport inhibition, auxin signalling and perception, thereby influencing plant resistance to pathogenic infection (Navarro *et al*., 2006). The remaining six differentially expressed transcripts were down-regulated (Table 4.8).

4.4.4.1 Target gene expression per data set

The 2015 2 GH data set yielded three differentially expressed target genes (Table 4.8). Both miR156g targets are described as squamosa promotor-binding-protein-like (SPL) transcription factors. These transcription factors affect a wide range of plant developmental processes, including anthocyanin accumulation, leaf size and initiation rate (Gou *et al*., 2011; Wang *et al*., 2011b). These genes are of interest, considering the changes in leaf morphology observed in GLD symptom expression. An additional miRNA target gene (miR397a_target) showed notable changes in expression levels [log$_2$ (fold change) value of -1.262] between diseased and healthy samples, though statistical significance could not be ascribed to these differences. miR397a_target is described as a laccase-4-like protein located in the apoplast, and is implicated in oxidation-reduction processes (Table 4.6). Reactive

oxygen species (ROS) accumulation in the apoplast is a primary, universal part of plant cell defence against biotic stresses (Bolwell *et al*., 2002; Gutha *et al*., 2010; Sgherri *et al*., 2013). Metabolites such as ascorbate, glutathione and tocopherols (containing hydroquinone elements) form part of antioxidant systems which prevent over-production of ROS (Pignocchi *et al*., 2006; Sgherri *et al*., 2013; Szarka *et al*., 2012). Most laccase proteins targeted by miR397a were predicted to be involved in oxidation-reduction processes in the apoplast (Addendum B). De Tullio *et al*. (2013) suggested a miRNA-mediated regulation of ascorbate oxidase in apoplastic oxidation-reduction processes. The consistent modulation of miR397a in GLRaV-3 infected plants across all data sets, coupled with the notable modulation of its target gene, suggests that this miRNA and its targets may play an important role in GLRaV-3 plant-pathogen interaction.

Four miRNA target genes showed differential expression in the 2016 field data set (Table 4.8). The significant down-regulation of miR162_target (Disease resistance rpp13-like protein 1) in diseased plants could suggest a suppression of host defence systems. Bester *et al*. (2016) reported differential expression of a gene (GSVIVT01024634001) targeted by a known plant homologue of vvi-miR408 in GLRaV-3 infected grapevine. The sequence of this target was highly similar to that of a phagocyte signalling protein implicated in actin cytoskeleton organisation, transport processes and innate immunity (Henty-Ridilla *et al*., 2013). The only genes that were differentially expressed in both data sets were targeted by miR393a. The regular involvement of miR393a and its predicted targets in GLRaV-3 infection is in agreement with various studies on plant biotic stress response (Navarro *et al*., 2006; Ruiz-Ferrer and Voinnet, 2009). The targets for miR166h are homeobox leucine zipper proteins and have been shown to be key regulators for normal plant growth and development (Elhiti and Stasolla, 2009; Singh *et al*., 2014). The down-regulation of miR166h_target (Homeobox leucine zipper ATHB-15) in diseased plants could contribute to the stunted growth and developmental defects observed in GLD symptomatic grapevine.

The target gene expression trends in the 2016 field data set were similar to that of the miRNA quantitation results for this data set. Plants from farm B contributed the most to the statistical significance of differences observed between diseased and healthy plants. This is evident when considering the p-values of diseased versus healthy samples per farm, across the four differential miRNA targets (Table 4.9). The greater miRNA target response in plants that could have been infected for longer is in agreement with miRNA quantitation results (Table 4.9) and suggests a greater plant response to a more established GLRaV-3 infection. The expression of miR397a_target in the 2016 field data set could not be determined due to insufficient amplification for standard curve construction. The abundance of this gene could have been too low for accurate quantitation, which

44

would correlate with the down-regulation of this target in the 2015 2 GH data set, though this was not validated.

Table 4.9 Differentially expressed miRNAs and targets per farm in the field 2016 data set.

miRNAs	Overall			Per farm	
	P-value	log$_2$ (fold change)[a]	Farms	P-value	log$_2$ (fold change)[a]
miR408	0.005518	-0.9884125	Farm A	0.7546	-0.2117803
			Farm B	0.0002733*	-1.38196
miR397a	1.461e-06	-1.733065	Farm A	0.004662	-1.480167
			Farm B	0.0002111*	-1.87673
miR398b	0.0001185	-1.517534	Farm A	0.4136	-0.612165
			Farm B	2.906e-05*	-1.839318
miRNA targets					
miR408_target	0.02378	-0.620384	Farm A	0.1079	-0.9594338
			Farm B	0.02117*	-0.5742253
miR393a_target 1	0.02013	-0.1743746	Farm A	0.08125	-0.2364747
			Farm B	0.1553	-0.1557787
miR166h_target	0.0009219	-0.2860509	Farm A	0.04262	-0.347897
			Farm B	0.02117*	-0.2567138
miR162_target	0.04124	-0.5860558	Farm A	0.2824	-0.4163815
			Farm B	0.0009774*	-0.698612

* Instances in which the down-regulation in plants from farm B was more pronounced than farm A.
[a] log$_2$ (fold change) was calculated as diseased/healthy.

4.4.4.2 Target gene expression between single-variant infections in greenhouse plants

The expression of miRNA target genes varied between different variant group infections, though not to the same extent as for miRNA expression levels. Variant groups VI and VII showed statistically significant differences in all three differentially expressed target genes in this data set. For miR397_target, variant group VII infections showed a markedly higher expression modulation than other variant group infection [log$_2$ (fold change) of -2.421] when comparing diseased versus healthy plants per group. Variant group II showed the highest degree of differential expression when comparing target gene expression levels between variant group infections. This variant group also had the highest calculated VCRs in this data set (Figure 4.4), which suggests a correlation between miRNA target gene expression and virus concentration. No statistically significant differences in miRNA target gene expression was observed between single-variant and mixed-variant infected plants of the 2016 field data set.

45

No significant anti-correlation relationships between the expression of miRNAs and their predicted target genes were observed in the two data sets. This can be explained by the fact that these miRNAs were predicted to target multiple transcripts, of which we selected only one (two in some instances) to screen. It is possible that a different miRNA target gene was acted upon in GLRaV-3 infection than the target that was screened for. Additionally, *in silico* tools for miRNA target prediction have been shown to produce more false positive predictions in plants other than the model organism, *A. thaliana* (Srivastava *et al*., 2014). Understanding the miRNA-target interaction is confounded by factors such as individual miRNAs having multiple target genes (Jones-Rhoades and Bartel, 2004; Pasquinelli 2012), and the possible conjunctional regulation of the same target gene by multiple miRNAs (Bulow *et al*., 2012).

Chapter 5: Conclusions

The grapevine industry has global economic importance, however, its susceptibility to virus infection, and the resulting negative effects of the associated disease complexes, threaten its sustainability. Grapevine leafroll disease (GLD) is arguably the most economically important disease of the five viral disease complexes, and is primarily caused by infection with grapevine leafroll-associated virus 3 (GLRaV-3). No natural source of resistance to GLD has been identified to date. This lack of resistance, coupled with challenges in creating disease resistance by conventional breeding approaches requires the development and use of innovative disease management strategies (Naidu *et al*., 2014). Developing such effective management strategies requires knowledge of the molecular interaction between the plant and the virus. Plant sRNAs, such as miRNAs, have been shown to mediate gene regulation in nearly all aspects of plant functioning, including biotic stress responses such as virus infection. It is therefore possible that plant sRNAs can play a role in the plant's defence response to GLRaV-3 infection. In this study we aimed to characterise the plant response to GLRaV-3 infection by investigating the expression of miRNAs and their putative target genes between diseased and healthy samples. Virus concentrations were also calculated and compared between the four data sets. The availability of GLRaV-3 single-variant infected plants allowed for additional comparisons relating to the genetic variability of GLRaV-3, and the possible biological distinctions between virus variants. Plants grown under greenhouse and field conditions were included to ensure that environmental factors influencing grapevine growth and disease dynamics were taken into account.

The expression of nine miRNAs was investigated in GLRaV-3 infected plants in four data sets using a probe-based RT-qPCR approach. These miRNAs were chosen based on their reported modulation in GLD symptomatic grapevine (Alabi *et al*., 2012; Bester *et al*., 2016). Several miRNAs were significantly differentially expressed across the four data sets (Table 4.5). The miRNAs that showed the most consistent differential expression in GLRaV-3 infected plants were miR408, miR398b, miR397a and miR162. The direction of regulation, i.e. up- or down- regulation for each miRNA in the diseased state was not consistent across all data sets, indicating that these miRNAs do not form part of a possible universal response to GLRaV-3 infection. This finding highlights the complexity of miRNA regulation in plant virus infection. The regular modulation of miR398b in this study is in agreement with various studies that strongly implicate the miR398 family in plant stress responses. The only miRNA that showed notable expression modulation in all four data sets was miR397a. The consistent differential expression of miR397a in GLRaV-3 infection in this study, and the functions of its putative target genes (laccase enzymes) are aligned with current perspectives on plant biotic

stress and is an encouraging finding. These results suggest that miR397a is likely involved in the GLRaV-3 stress response.

MicroRNA expression between GLRaV-3 variant group infections varied, as the same miRNA would be up-regulated in some variant groups and down-regulated in others. The most significant example of this is miR393a, which showed this varying trend of miRNA regulation between variant group infections across all data sets. miR393a was predicted to target genes involved in protein transport inhibition and auxin signalling and perception, thereby affecting plant resistance to pathogenic infection. Various studies on plant biotic stress have reported differential expression of the miR393 family. The modulation of miR393a and differential expression of its target genes in both the 2015 GH and 2016 field data sets suggest that this miRNA and its targets play a role in the GLRaV-3 stress response. Additionally, the expression of miR393a in this study indicates a possible variant-specific response to GLRaV-3 infection and warrants further investigation. MicroRNA expression in variant group VII infections was often shown to differ the most from other variant groups, and statistically significant differences in expression were observed in many instances, mostly relative to variant groups I and II. The higher calculated VCRs of variant groups I and II compared to group VII, and the differential miRNA regulation observed between these groups is an intriguing result. A possible correlation can be made between miRNA expression in variant group VII infected plants and lower VCRs observed for this variant group across all data sets. The fact that variant group VII is the most divergent variant investigated, coupled with lower calculated VCRs and dissimilar miRNA expression could indicate a more effective plant response to infection with this variant. Evaluating how this sequence variation possibly translates to differences in the host-pathogen interaction could yield valuable insights into the biological properties of GLRaV-3 variants and possible differences in pathogenicity.

Substantial variation in miRNA expression between the different data sets was observed. Plants from these data sets differed in terms of growing conditions, scion/rootstock combination, age and duration of infection. We therefore compared the miRNA expression observed per data set, to relate the differences observed to these plant differences. The expression of miRNAs in GLRaV-3 infection was found to be more pronounced in own-rooted plants compared to plants that were grafted onto rootstocks, in greenhouse trials. This correlates with recent findings in our research group (Bester *et al*., 2016 unpublished), in which NGS was used for sRNA profiling of different *V. vinifera* cultivars in response to GLRaV-3 variant group II infection. The fact that the different approaches of expression profiling delivered comparable results in terms of miRNA expression in GLRaV-3 infected plants is promising and necessitates further investigation. Only two rootstock cultivars, 101-

14 and Richter 110, were utilised in this study (Table 3.1). Including more rootstock cultivars in future studies on sRNA expression in GLRaV-3 infection could yield important insights into why these grafting-related differences in miRNA regulation exist. Such studies could also aid in characterising the molecular basis for reported differences in the effects of GLD in grafted red-fruited cultivars of varying scion/rootstock combinations.

The two data sets that showed the highest degree of differential miRNA expression, 2014 GH and 2016 field (Table 4.5), consisted of plants established several years before the 2015 GH data sets. The plants from the 2014 GH data set were cuttings from established symptomatic infections, whereas the plants from the 2016 field data set were likely infected with GLRaV-3 for longer than the 2015 GH data set, given the age of the plants. This effect on miRNA expression was also evident between farms of the 2016 field data set in which vineyard blocks in farm B showed a higher degree of differential miRNA modulation (Figure 4.5). The vineyards from farm B were established before the vineyards from farm A, and generally these plants could have been infected with GLRaV-3 for longer. The expression of miRNA target genes showed similar trends between the two farms (Table 4.9). These results indicate a more substantial miRNA/target response in plants having a longer and more established infection of GLRaV-3.

The expression of *in silico* predicted miRNA target genes was evaluated using an RT-qPCR assay. Several miRNA targets showed significant expression modulation between diseased and healthy samples in the two data sets, 2015 2 GH and 2016 field (Table 4.8). The descriptions and gene ontology (GO) annotations of these targets are in agreement with recent reports of differential gene expression in grapevine virus infections. These differentially expressed targets can also be used in future grapevine functional studies and contribute to the establishment of novel disease management strategies.

Differences in virus concentration between GLRaV-3 variant infections have not been fully validated. A SYBR Green RT-qPCR assay was used to determine the relative concentration of GLRaV-3, expressed as virus concentration ratios (VCRs), in all samples. Plants infected with variant groups I and II showed significantly higher VCRs compared to groups VI and VII. Statistically significant differences in VCRs were calculated in several instances (Table 4.3). Interestingly, no significant differences in mean VCRs of each data set were observed (Figure 4.3), despite considerable differences in the plant age and duration of GLRaV-3 infection. This finding suggests that the effects of GLRaV-3 over time do not necessarily correspond with the abundance of the virus within the plant. These results could also indicate that plant defence mechanisms were successful in inhibiting further

virus replication over time. The greater miRNA response observed in plants with more established infections is therefore a promising result and warrants further investigation. The fact that the same miRNAs (miR398b, miR397a and miR408) were differentially expressed in the two data sets that were likely infected with GLRaV-3 for longer (2014 GH and 2016 field) suggests that these miRNAs may be directly involved in defence mechanisms inhibiting GLRaV-3 replication.

Limitations of this study included the relatively small panel of miRNAs that were investigated in the four data sets. Expanding the number of miRNAs investigated in future studies will aid in further elucidating the molecular interactions underlying GLRaV-3 infection. Likewise, the number of miRNA targets screened was relatively low (roughly one target gene per miRNA). This could be a contributing factor to the lack of significant anti-correlation observed between miRNAs and their targets in this study. Factors such as individual miRNAs targeting multiple genes, and single target genes possibly co-regulated by multiple miRNAs, complicate the understanding of miRNA-target interactions. An NGS approach combining sRNA expression profiles and transcriptome data, followed by qPCR validation, could likely circumvent these limitations, as shown by Bester *et al*. (2016). The aforementioned study only utilised GLRaV-3 variant group II and therefore the set of single-variant infected greenhouse plants (2015 GH) that was established in this study is a valuable resource for further investigations on GLRaV-3 variants and their biological properties.

Furthermore, expanding the sampling to different physiological/phenological stages to enable comparisons could prove insightful. Grapevine leafroll disease is unique in that symptom expression, or the lack thereof, corresponds in broad terms to two distinct phenological stages. miRNA expression has also been shown to differ in various tissue types and in different physiological growth stages (Kullan *et al*., 2015). It would be of interest to evaluate miRNA expression in GLD in pre-véraison and at véraison, to see if any expression changes occur with symptom development. This will aid in elucidating the mechanisms underlying GLD symptom development, and may shed light on why some cultivars remain asymptomatic.

References

Afzal, A. J., Wood, A. J. and Lightfoot, D. A. (2008) Plant receptor-like serine threonine kinases: roles in signalling and plant defense. *Mol. Plant Microbe Interact.* **21**:507–517. doi: 10.1094 / MPMI -21-5-0507.

Agranovski, A. A., Koonin, E. V., Boyko, V. P, Frötschl, N. A., Lunina, N. A. and Atabekov, J. G. (1994) Beet yellows closterovirus: Complete genome structure and identification of a leader papain-like thiol protease. *Virology.* **198**:311 – 324. doi: http://dx.doi.org/10.1006/viro.1994.1034.

Alabi, O. J., Zheng, Y., Jagadeeswaran, G., Sunkar, R. and Naidu, R. A. (2012) High-throughput sequence analysis of small RNAs in grapevine (*Vitis vinifera* L.) affected by grapevine leafroll disease. *Mol. Plant. Pathol*. **13**(9): 1060-1076.

Alabi, O. J., Casassa, L. F., Gutha, L. R., Larsen, R. C., Henick-Kling, T., Harbertson, J. F., Naidu, R. A. (2016) Impacts of Grapevine Leafroll Disease on Fruit Yield and Grape and Wine Chemistry in a Wine Grape (Vitis vinifera L.) Cultivar. *PlosOne*. **11**(2):e0149666 http://dx.doi.org/10.1371/journal.pone.0149666.

Almeida, R. P. P., Daane, K. M., Bell, V. A., Blaisdell, G. K., Cooper, M.L., Herrbach, E. and Pietersen, G. (2013) Ecology and management of grapevine leafroll disease. *Front. Microbiol*. **4**: Article 94.

Al Rwahnih, M., Daubert, S., Golino, D., Islas, C. and Rowhani, A. (2015) Comparison of Next-Generation Sequencing versus biological indexing for optimal detection of viral pathogens in grapevine. *Phytopathol*. **105**(6):758-763.

Atallah, S., Gomez, M., Fuchs, M. and Martinson, T. (2012) Economic impact of grapevine leafroll disease on Vitis vinifera cv. Cabernet franc in Finger Lakes vineyards of New York. *Am. J. Enol. Vitic*. **63**: 73-79.

Axtell, M. J. (2013) Classification and comparison of small RNAs from plants. *Annu Rev Plant Biol.* **64**:137– 159. doi: 10.1146/annurev-arplant-050312-120043.

Basso, M. F., Fajardo, T. V. M., Santos, H. P., Guerra, C. C., Ayub, R. A. and Nickel, O. (2010) Leaf physiology and enologic grape quality of virus-infected plants. *Trop. Plant Pathol*. **35**: 351-59.

Bazzini, A. A, Hopp, H. E., Beachy, R. N. and Asurmendi, S. (2007) Infection and coaccumulation of tobacco mosaic virus proteins alter microRNA levels, correlating with symptom and plant development. *Proc. Natl. Acad. Sci. USA*. **104**(29): 12157–12162.

Bazzini, A. A., **Almasia, N. I.**, **Manacorda, C. A.**, **Mongelli, V. C.**, **Conti, G.**, **Maroniche, G. A.**, **Rodriguez, M. C.**, **Distéfano, A. J.**, **Hopp, H. E.**, **Vas, M. and Asurmendi, S.** (2009) Virus infection elevates transcriptional activity of miR164a promoter in plants. *BMC Plant Biol.* **9**: 152.

Bertamini, M., and Nedunchezhian, N. (2002) Leaf age effects on chlorophyll, Rubisco, photosynthetic electron transport activities and thylakoid membrane protein in field grown grapevine leaves. *J. Plant Physiol*. **159**: 799-03.

Bertamini, M., Muthuchelian, K. and Nedunchezhian, N. (2004) Effect of Grapevine Leafroll on the Photosynthesis of Field Grown Grapevine Plants (Vitis vinifera L. cv. Lagrein). *J Phytopathol*. **152**:145-52.

Bester, R., Maree, H. J. and Burger, J. T. (2012a) Complete nucleotide sequence of a new strain of grapevine leafroll-associated virus 3 in South Africa. *Arch. Virol*. **157**:1815–1819.

Bester, R., Jooste, A. E. C., Maree, H. J. and Burger, J. T. (2012b) Real-time RT-PCR high-resolution melting curve analysis and multiplex RT-PCR to detect and differentiate grapevine leafroll-associated virus 3 variant groups I, II, III and VI. *Virol. J*. **9**: 219.

Bester, R., Pepler, P.T., Burger, J.T. and Maree, H.J. (2014) Relative quantitation goes viral: An RT-qPCR assay for a grapevine virus. *J. Virol. Methods.* **210**: 67-75.

Bester, R., Burger, J. T. and Maree, H. J. (2016) Differential expression of miRNAs and associated gene targets in grapevine leafroll-associated virus 3 infected plants. *Arch. Virol*. (Accepted).

Bester, R., Pepler, P. T., Aldrich, D. J. and Maree, H. J. (2017) Harbin: A quantitation PCR analysis tool. *Biotechnol. Lett*. **39**(1):171-178.

Blaisdell, G. K., Zhang, S., Daane, K. and Almeida, R. P. P. (2012) "Patterns of virus transmission from hosts with mixed infections," in *Proceedings of the 17thCongress of ICVG7–14October (Davis: Foundation Plant Services)*. 178–179.

Blaisdell, G. K., Zhang, S., Bratburd, J. R., Daane, K. M., Cooper, M. L. and Almeida, R. P. P. (2015) Interactions Within Susceptible Hosts Drive Establishment of Genetically Distinct Variants of an Insect-Borne Pathogen. *J. Econ. Entomol*. **108**(4):1531-1539.

Bolwell, P. P., Page, A., Piglewska, M. and Wojtaszek, P. (2001) Pathogenic infection and the oxidative defences in plant apoplast. *Protoplasma*. **217**:20-32.

Bolwell, G. P., Bindschedler, L. V., Blee, K. A., Butt, V. S. and Minibayeva, F. (2002) The apoplastic oxicative burst in response to biotic stress in plants: a three-component system. **53** (372): 1367-1376.

Bulow, L., Bolivar, J. C., Ruhe, J., Brill, Y. and Hehl, R. (2012) 'MicroRNA Targets', a new AthaMap web-tool for genome-wide identification of miRNA targets in Arabidopsis thaliana. *BioData Min*. **5**: 7.

Cabaleiro, C., Segura, A. and GarcÍa-Berrios, J. J. (1999) Effects of Grapevine Leafroll-Associated Virus 3 on Physiology and Must of *Vitis vinifera* L. cv. Albariño Following Contamination in the Field. *Am. J. Enol. Vitic*. **50**(1): 40-44.

Cabaleiro, C., and Segura, A. (2006) Temporal analysis of grapevine leafroll associated virus 3 epidemics. *Eur. J. Plant Pathol*. **114**: 441-446.

Carra, A., Gambino, G. and Schubert, A. (2007) A cetyltrimethylammonium bromide-based method to extract low-molecular-weight RNA from polysaccharide-rich plant tissues. *Anal. Biochem*. **360**: 318-320.

Charles, J. G., Cohen, D., Walker, J. T. S., Forgie, S. A., Bell, V. A. and Breen, K. C. (2006) A review of the ecology of grapevine leafroll associated virus type 3 (GLRaV-3). *N Z Plant Prot.* **59**:330–337.

Charles, J. G., Froud, K. J., van den Brink, R. and Allan, D. J. (2009) Mealybugs and the spread of grapevine leafroll-associated virus 3 (GLRaV-3) in a New Zealand vineyard. *Australas. Plant. Pathol.* **38**:576–583. doi:10.1071/AP09042.

Chen, C., Ridzon, D. A., Broomer, A. J., Zhaohui, Z., Lee, D. H., Nguyen, J. T., Barbisin, M., Xu, N. L., Mahuvakar, V. R., Andersen M. R., Lao, K. Q., Livak, K. J. and Guegler, K. J. (2005) Real-time quantification of microRNAs by stem-loop RT-PCR. *Nucleic Acids Res*. **33**(20):e179.

Chooi, K. M., Cohen, D. and Pearson, M. N. (2013a) Molecular characterisation of two divergent variants of Grapevine leafroll-associated virus 3 in New Zealand. *Arch. Virol*. doi:10.1007/s00705-013-1631-9.

Chooi, K. M., Cohen, D. and Pearson, M. N. (2013b) Generic and sequence-variant specific molecular assays for the detection of the highly variable Grapevine leafroll-associated virus 3. *J. Virol. Methods*. **189**:20–29.

Chuck, G., and O'Connor, D. (2010) Small RNAs going the distance during plant development. *Curr. Opin. Plant Biol*. **13**: 40-45.

Coetzee, B., Freeborough, M., Maree, H. J., Celton, J., Rees, D. J., and Burger, J. T. (2010). Deep sequencing analysis of viruses infecting grapevines: virome of a vineyard. *Virology*. **400**: 157–163.

Conesa, A. and Götz, S. (2008) Blast2GO: A Comprehensive Suite for Functional Analysis in Plant Genomics. *Int. J. Plant Genomics.* 1–12. doi: 10.1155/2008/619832.

Cookson, S. J. and Ollat, N. (2013) Grafting with rootstocks induces extensive transcriptional re-programming in the shoot apical meristem of grapevine. *BMC Plant Biol.* **13**:147. doi: 10.1186/1471-2229-13-147 PMID: 24083813.

Dai, X. and Zhao, P. X. (2011) psRNATarget: a plant small RNA target analysis server. *Nucleic Acids Res.* **39**:W155–W159. doi: 10.1093/nar/gkr319.

Demangeat, G., Komar, V., Van-Ghelder, C., Voisin, R., Lemaire, O., Esmenjaud, D. and Fuchs, M. (2010) Transmission competency of singlefemale Xiphinema index lines for Grapevine fanleaf virus. *Phytopathology.* **100**:384-389.

De Tullio, M. C., Guether, M. and Balestrini R. (2013) Ascorbate oxidase is the potential conductor of a symphony of signaling pathways. *Plant Signal. Behav*. **8**: e23213.

Elhiti, M. and Stasolla, C. (2009) Structure and function of homodomain-leucine zipper (HD-Zip) proteins. *Plant Signal Behav.* **4**:86–88.

Engel, E. A., Girardi, C., Escobar, P. F., Arredondo, V., Dominguez, C., Pérez-Acle, T. and Valenzuela, P. D. T. (2008) Genome analysis and detection of a Chilean isolate of Grapevine leafroll associated virus-3. *Virus Genes*. **37**(1):110–118.

Engel, E. A., Escobar, P. F., Rojas, L. A., Rivera, P. A., Fiore, N. and Valenzuela, P. D. (2010) A diagnostic oligonucleotide microarray for simultaneous detection of grapevine viruses. *J. Virol. Methods.* **163**:445–451. doi: 10.1016/j.jviromet.2009.11.00.

Espinoza, C., Vega, A., Medina, C., Schlauch, K., Cramer, G. and Arce-Johnson, P. (2007a) Gene expression associated with compatible viral diseases in grapevine cultivars. *Funct. Integr. Genomics*. **7**: 95-110.

Espinoza, C., Medina, C., Somerville, S. and Arce-Johnson, P. (2007b) Senescence-associated genes induced during compatible viral interactions with grapevine and Arabidopsis. *J. Exp. Bot*. **58**: 3197-12.

FAO (2012) Food and Agriculture Organization of the United Nations 1182 Plant Disease / Vol. 98 No. 9 FAOSTAT-Agriculture. http://faostat3.fao.org/faostat-gateway/go/to/home/E. (2 December 2016)

Farooq, A. B. U., Ma, Y., Wand, Z., Zhou, N. and Wenxing, X. (2013) Genetic diversity analyses reveal novel recombination events in Grapevine leafroll-associated virus-3 in China. *Virus Res*. **171**: 15–21.

Freeborough, M. -J., and Burger, J. (2006) Leaf roll: Economic implications. *Wynboer*. http://www.wynboer.co.za/ recentarticles/200812-leafroll.php3.

Fuchs, M., Martinson, T. E., Loeb, G. M. and Hoch, H. C. (2009) Survey for the three major leafroll disease-associated viruses in Finger Lakes vineyards in New York. *Plant Dis*. **93**:395–401.

Goodall, E. F., Heath, P. R., Bandmann, O., Kirby, J. and Shaw, P. J. (2013) Neuronal dark matter: the role of microRNAs in neurodegeneration. *Font. Cell. Neurosci*. **7**:178. doi:10.3389/fncel.2013.00178.

Goszczynski, D. E. (2013) Brief report of a new highly divergent variant of grapevine leafroll-associated virus 3 (GLRaV-3). *J. Phytopath*. **161**(11–12): 874–879.

Gou, J. Y., Felippes, F. F., Liu, C. J., Weigel, D. and Wang, J. W. (2011) Negative regulation of anthocyanin biosynthesis in Arabidopsis by a miR156-targeted SPL transcription factor. *Plant Cell*. **23**: 1512–1522.

Gouveia, P., Santos, M. T., Eiras-Dias, J. E. and Nolasco, G. (2011) Five phylogenetic groups identified in the coat protein gene of grapevine leafroll-associated virus 3 obtained from Portuguese grapevine varieties. *Arch. Virol*. **156** (3):413–420.

Guleria, P., Mahajan, M., Bhardwaj, J. and Yadav, S. K. (2011) Plant Small RNAs: Biogenesis, Mode of Action and Their Roles in Abiotic Stresses. *Genomics Proteomics Bioinformatics*. **9**(9): 183-199.

Gutha, L. R., Casassa, L. F., Harbertson, J. F. and Naidu, R. A. (2010) Modulation of flavonoid biosynthetic pathway genes and anthocyanins due to virus infection in grapevine (*Vitis vinifera* L.) leaves. *BMC Plant Biol*. **10**: 187.

Gutha, L. R., Alabi, O. J. and Naidu, R. A. (2012) Effects of grapevine leafroll disease on photosynthesis in a red-fruited wine grape cultivar. *Proc. 17th Congr. Internatl. Counc. Study of Virus and Virus-like Dis. Grapevine (ICVG)*, Davis, California, USA, Oct. 7-14, pp.168- 69.

He, F., Mu, L., Yan, G. L., Liang, N. N., Pan, Q. H., Wang, J., Reeves, M. J. and Duan, C. Q. (2010) Biosynthesis of anthocyanins and their regulation in colored grapes. *Molecules*. **15**: 9057-91.

Henty-Ridilla, J. L., Shimono, M., Li, J., Chang, J. H., Day, B. and Staiger, C. J. (2013) The Plant Actin Cytoskeleton Responds to Signals from Microbe-Associated Molecular Patterns**. *PLOS Pathog* **9**:e1003290. doi: 10.1371/journal.ppat.1003290.

Hoskins, N., Thompson, C. and Andrew, R. (2011) New Zealand Winegrowers working hard to eliminate leafroll. *Aust. N.Z. Grapegrow. Winemak*. **569**: 23–25.

Iwakawa, H. and Tomari, Y. (2015) The Functions of MicroRNAs: mRNA Decay and Translational Repression. *Trends Cell Biol*. **25**(11):651-665.

Jensen, P. J., Makalowska, I., Altman, N., Fazio, G., Praul, C., Maximova, S. N., Crassweller, R. M., Travis, J.W. and McNellis, T. W. (2010) Rootstock-regulated gene expression patterns in apple tree scions. *Tree Genet. Genomes*. **6**(1): 57-72. 10.1007/s11295-009-0228-7.

Jones, T. H., Cullis, B. R., Clingeleffer, P. R. and Ruhl, E. H. (2009) Effects of novel hybrid and traditional rootstocks on vigour and yield components of Shiraz grapevines. *Aust. J. Grape Wine Res*. **15** (3): 284-292. 10.1111/j.1755-0238.2009.00061.x.

Jones-Rhoades, M. W. and Bartel, D. P. (2004) Computational identification of plant microRNAs and their targets, including a stress-induced miRNA. *Mol Cell*. **14**:787- 99

Jooste A. E. C, Maree, H. J., Bellstedt, D. U., Goszczynski, D. E., Pietersen, G. and Burger, J. T. (2010) Three genetic grapevine leafroll-associated virus 3 variants identified from South African vineyards show high variability in their 5'UTR. *Arch. Virol*. **155**:1997–2006.

Jooste, A. E. C., Pietersen, G. and Burger, J. T. (2011) Distribution of grapevine leafroll associated virus-3 variants in South African vineyards. *Eur. J. Plant Pathol*. **131**(3):371-381.

Jooste, A. E. C., Bester, R., Maree, H.J., de Koker, W. and Burger, J.T. (2012) A Survey of Red and White Cultivars to Test an Improved Detection Technique for Grapevine Leafroll-Associated Virus 3 (GLRaV-3) Variants Identified in South African Vineyards. *Proceedings of the 17th Congress of ICVG*. 122-123.

Jooste, A.E.C., Molenaar, N., Maree, H.J., Bester, R., Morley, L., de Koker, W. C. and Burger, J. T. (2015) Identification and distribution of multiple virus infections in Grapevine leafroll diseased vineyards. *Eur. J. Plant Pathol*. **142**(2):363-375

Kertesz, M., Iovino, N., Unnerstall, U., Gaul, U. and Segal, E. (2007) The role of site accessibility in microRNA target recognition. *Nat Genet*. **39**(10):1278-84.

Khraiwesh, B., Zhu, J. K and Zhu, J. (2012) Role of miRNAs and siRNAs in biotic and abiotic stress responses of plants. *Biochim. Biophys. Acta*. **1819**: 137-148.

King, A. M. Q., Lefkowitz, E., Adams, M. J. and Carstens, E. B. (2011) Virus Taxonomy: Ninth Report of the International Committee on Taxonomy of Viruses. Elsevier Science Comparison of Next-Generation Sequencing Versus Biological Indexing for the Optimal Detection of Viral Pathogens in Grapevine. *Phytopathology*.

Komar, V., Vigne, E., Demangeat, G., Lemaire, O. and Fuchs, M. (2010) Comparative performance analysis of virus-infected Vitis vinifera cv. Savagnin rose grafted onto three rootstocks. *Am. J. Enol. Vitic.* **61**: 68–73.

Kreuze, J. F., Perez, A., Untiveros, M., Quispe, D., Fuentes, S., Barker, I. and Simon, R. (2009). Complete viral genome sequence and discovery of novel viruses by deep sequencing of small RNAs: a generic method for diagnosis, discovery and sequencing of viruses. *Virology.* **388:** 1–7.

Kullan, J. B., D L P Pinto, D. L. P., Bertolini, E., Fasoli, M., Zenoni, S., Tornielli, G. B., Pezzotti, M., Meyers, B. C., Farina, L., Pè, M. E. and Mica, E. (2015) miRVine: a microRNA expression atlas of grapevine based on small RNA sequencing. *BMC Genomics.* **16**:393. DOI: 10.1186/s12864-015-1610-5.

Kumar, S., Baranwal, V. K., Singh, P., Jain, R. K., Sawant, S., and Singh, S. K. (2012) Characterization of a Grapevine leafroll-associated virus 3 from India showing incongruence in its phylogeny. *Virus Genes.* **45**:195–200.

Lee, J. and Martin, R. R. (2009) Influence of grapevine leafroll associated viruses (GLRaV-2 and -3) on the fruit composition of Oregon Vitis vinifera L. cv. Pinot noir: Phenolics. *Food Chem.* **112**: 889–896.

Lee, J., Keller, K. E., Rennaker, C. and Martin, R. R. (2009) Influence of grapevine leafroll associated viruses (GLRaV-2 and -3) on the fruit composition of Oregon Vitis vinifera L. cv. Pinot noir: free amino acids, sugars, and organic acids. *Food Chem*. **117**: 99–105.

Ling, K. S., Zhu, H. Y., Drong, R. F., Slightom, J. L., McFerson, J. R. and Gonsalves, D. (1998) Nucleotide sequence of the 3'-terminal two-thirds of the grapevine leafroll-associated virus-3 genome reveals a typical monopartite closterovirus. *J. Gen. Virol.* **79**:1299–1307.

Ling, K., Zhu, H. and Gonsalves, D. (2004) Complete nucleotide sequence and genome organization of Grapevine leafroll-associated virus 3, type member of the genus Ampelovirus. *J. Gen. Virol*. **85**:2099–2102.

Liu, M. -H., Li, M. -J., Qi, H. -H., Guo, R., Liu, X. M., Wang, Q. and Cheng, Y. -Q. (2013) Occurrence of Grapevine leafroll-associated viruses in China. *Plant Dis*. **97**: 1339–1345.

MacKenzie, D. J. (1997) A standard protocol for the detection of viruses and viroids using reverse transcription-polymerase chain reaction technique. Document CPHBT-RT-RPCR1.00 *The Canadian food inspection Agency*.

Mannini, F., Mollo, A. and Credi, R. (2012) Field performance and wine quality modification in a clone of Vitis vinifera cv. Dolcetto after GLRaV-3 elimination. *Am. J. Enol. Vitic.* **63**: 144–147.

Maree, H. J., Freeborough, M. and Burger, J. T. (2008) Complete nucleotide sequence of a South African isolate of grapevine leafroll-associated virus 3 reveals a 5'UTR of 737 nucleotides. *Arch. Virol*. **153**:755–757.

Maree, H. J., Almeida, R. P. P., Bester, R., Chooi, K. M., Cohen, D., Dolja, V. V., Fuchs, M. F., Golino, D. A., Jooste, A. E. C., Martelli, G. P., Naidu, R. A., Rowhani, A., Saldarelli, P. and Burger, J. T. (2013) Grapevine leafroll-associated virus 3. *Front. Microbiol*. **4**: Article 82.

Maree, H. J., Pirie, M. D., Oosthuizen, K., Bester, R., Rees, J. G. and Burger, J. T. (2015) Phylogenomic Analysis Reveals Deep Divergence and Recombination in an Economically Important Grapevine Virus. *PLOS ONE* **10**:e0126819. doi: 10.1371/journal.pone.0126819.

Martelli, G. P. (2000) Major graft transmissible diseases of grapevines: Nature, diagnosis, and sanitation. *Proceedings of the ASEV 50th Anniversary Annual Meeting* 19–23 June, Seattle,WA.

Martelli, G. P., Agranovsky, A. A., Bar-Joseph, M., Boscia, D., Candresse, T., Coutts, R. H., Dolja, V. V., Falk B. W., Gonsalves, D., Jelkmann, W., Karasev, A. V., Minafra, A. Namba, S., Vetten, H. J., Wisler, G. C. and Yoshikawa, N. (2002) The family Closteroviridae revised. *Arch. Virol*. **147**(10): 2039–2044.

Martelli, G. P., Agranovsky, A. A. Bar- Joseph, M., Boscia, D., Candresse, T. et al. (2011) "Family Closteroviridae," in Virus Taxonomy. *Ninth Report of the International Committee on Taxonomy of Viruses,* eds A. King, M. J. Adams, E. B. Carstens, and E. Lefkowitz (Amsterdam: Elsevier-Academic Press), 987–1001.

Martelli, G. P., Agranovsky, A. A., Al Rwahnih, M., Dolja, V. V., Dovas, C. I., Fuchs, M., Gugerli, P., Hu, J. S., Jelkmann, W., Katis, N. I., Maliogka, V. I., Melzer, M. J., Menzel, W., Minafra, A., Rott, M. E., Rowhani, A., Sabanadzovic, S. and Saldarelli, P. (2012) Taxonomic revision of the family Closteroviridae with special reference to the grapevine leafroll-associated members of the genus Ampelovirus and the putative species unassigned to the family. *J. Plant Pathol*. **94**: 7–19.

Martelli, G. P. (2014) Directory of virus and virus-like diseases of the grapevine and their agents. *J. Plant Pathol*. **96**(Suppl. 1):1–136.

Martinson, T., Fuchs, M., Loeb, G. and Hoch, H. (2008) Grapevine Leafroll – an Increasing Problem in the Finger Lakes, the US and the World. *Cornell University Cooperative Extension*. (https://pdfs.semanticscholar.org/87ec/e318bc645f1ef28e4927dec32e8d9676d618.pdf).

Mendes, N. D., Freitas, A. T. and Sagot, M.-F. (2009) Current tools for the identification of miRNA genes and their targets. *Nucleic Acids Res*. **37**(8): 2419–2433.

Mishra, A. K., Duraisamy, G. S. and Matoušek, J. (2015) Discovering MicroRNAs and Their Targets in Plants. *CRC Crit. Rev. Plant Sci*. **34**(6): 553-571

Myles, S., Boyko, A. R., Brown, P. J., Grassi, F., Owens, C. L., Aradhya, M., Prins, B., Reynolds, A., Chia, J. M., Ware, D., Bustamante, C. D. and Buckler, E. S. (2011) Genetic structure and domestication history of the grape. *Proc. Natl. Acad. Sci*. **108**:3530-3535.

Naidu, R. A., O'Neil, S. and Walsh, D. (2008) Grapevine leafroll disease. *WSU Extension Bulletin* EB2027E.

Naidu, R., Rowhani, A., Fuchs, M., Golino, D. and Martelli, G. P. (2014) Grapevine leafroll: A Complex Viral Disease affecting a High-value Fruit Crop. *Plant Dis*. **98**(9): 1172-1185.

Naidu, R., Maree, H. J. and Burger, J. T. (2015) Grapevine leafroll disease and associated viruses: a unique pathosystem. Annu. Rev. Phytopathol. **53**(28)1-22.

Navarro, L., Dunoyer, P., Jay, F., Arnold, B., Dharmasiri, N., Estelle, M., Voinnet, O. and Jones, J. D. G. (2006) A plant miRNA contributes to antibacterial resistance by repressing auxin signaling. *Science*. **312**:436–439.

Nimmo-Bell (2006) The economic effects and financial impact of GLRaV3. A Nimmo-Bell Publication, March 2006.

OIV (2016) Organisation of Vine and Wine. (http://www.oiv.int/). (1 December 2016)

Pantaleo, V., Szittya, G., Moxon, S., Miozzi, L., Moulton, V., Dalmay, T. and Burgyan, J. (2010) Identification of grapevine microRNAs and their targets using high-throughput sequencing and degradome analysis. *Plant J*. **62**(6): 960-976.

Pasquinelli, A. E. (2012) MicroRNAs and their targets: recognition, regulation and an emerging reciprocal relationship. *Nat. Rev. Genet*. **13**: 271–282.

Pfaffl, M. W., Tichopad, A., Prgomet, C. and Neuvians, T. P. (2004) Determination of stable housekeeping genes, differentially regulated target genes and sample integrity: BestKeeper – Excel-based tool using pair-wise correlations. *Biotechnol. Lett*. **26**:509-515.

Pietersen, G. (2006) Spatio-temporal distribution dynamics of grapevine leafroll disease in Western Cape vine- yards, in *Extended abstracts of the 15th Meeting of the International Council for the Study of Virus and Virus-like diseases of the Grapevine (ICVG)*, April 3–7, Stellenbosch, South Africa, 126–127.

Pignocchi, C., Kiddle, G., Hernandez, I., Foster, S. J. and Asensi, A. (2006) Ascorbate Oxidase-Dependent Changes in the Redox State of the Apoplast Modulate Gene Transcript Accumulation Leading to Modified Hormone Signaling and Orchestration of Defense Processes in Tobacco. *Plant Physiol*. **141**: 423-435.

Pritchard, C. C., Cheng, H. H. and Tewari, M. (2012) MicroRNA profiling: approaches and considerations. *Nature Rev. Genet.* **13**:358-369.

Reid, K. E., Olsson, N., Schlosser, J., Peng, F. and Lund, S. T. (2006) An optimized grapevine RNA isolation procedure and statistical determination of reference genes for real-time RT-PCR during berry development. *BMC Plant Biol*. DOI: 10.1186/1471-2229-6-27.

Reinhart, B. J., Weinstein, E. G., Rhoades, M. W., Bartel, B. and Bartel, D. P. (2002) MicroRNAs in plants. *Genes Dev*. **16**: 1616-1626.

Sambrook, J., Frisch, E. F. and Maniates, T. (1989) Molecular cloning: a laboratory guide. *Cold Spring Harbour laboratory press*. Second edition. Cold Spring Harbor, New York.

Ruiz-Ferrer, V. and Voinnet, O. (2009) Roles of plant small RNAs in biotic stress responses. *Annu. Rev. Plant Biol*. **60**: 485–510.

SAWIS (2016) South African Wine Industry Statistics report nr. 40. SAWIS, Paarl (http://www.sawis.co.za/). (1 December 2016).

Schaad, N. W., Frederick, R. D., Shaw, J., Schneider, W. L., Hickson, R., Petrillo, M. D. and Luster, D. G. (2003) Advances in molecular-based diagnostics in meeting crop biosecurity and phytosanitary issues. *Annu. Rev. Phytopathol*. **41**:305–324.

Seah, Y. M., Sharma, A. M., Zhang, S., Almeida, R. P. P. and Duffy, S. (2012) A divergent variant of Grapevine leafroll-associated virus 3 is present in California. *Virol. J*. **9**: 235.

Sgherri, C., Ranieri, A. and Quartacci, M. F. (2013) Antioxidative responses *in Vitis vinifera* infected by grapevine fanleaf virus. *J. Plant Physiol*. **170**(2): 121-128.

Sharma, A. M., Wang, J., Duffy, S., Zhang, S., Wong, K. M., Rashed, A., Cooper, M. L., Daane, K. M. and Almeida, R. P. P. (2011) Occurrence of grapevine leafroll-associated virus complex in Napa Valley. *PLOS ONE*. **6**:e26227.

Singh, K., Talla, A. and Qiu, W. (2012) Small RNA profiling of virus-infected grapevines: evidences for virus infection-associated and variety-specific miRNAs. *Funct. Intergr. Genomics*. 12:659–669.

Singh, A., Singh, S., Panigrahi, K. C. S, Reski, R. and Sarkar, A. K. (2014) Balanced activity of microRNA166/165 and its target transcripts from the class III homeodomain-leucine zipper family regulates root growth in Arabidopsis thaliana. *Plant Cell Rep*. **33**:945–953. doi: 10.1007/s00299-014-1573-z.

Srivastava, P. K., Moturu, T. R., Pandey, P., Baldwin, I. T. and Pandey, S. P. (2014) A comparison of performance of plant miRNA target prediction tools and the characterization of features for genome-wide target prediction. *BMC Genomics*. **15**:348.

Sunkar, R. and Jagadeeswaran, G. (2008) In silico identification of conserved microRNAs in large number of diverse plant species. *BMC Plant Biol*. **8**:37.

Sunkar, R. (2010) MicroRNAs with macro-effects on plant stress responses. *Semin. Cell Dev. Biol*. **21**: 805–811.

Sunkar, R., Li, Y. and Jagadeeswaran, G. (2012) Functions of microRNAs in plant stress responses. *Trends Plant Sci*. **17**(4): 196-203.

Szarka, A., Tomasskovics, B. and Bánhegyi, G. (2012) The Ascorbate-glutathione-α-tocopherol Triad in Abiotic Stress Response. *Int. J. Mol. Sci*. **13**: 4458-4483.

Tagami, Y., Inaba, N., Kutsuna, N., Kurihara, Y. and Watanabe, Y. (2007) Specific enrichment of miRNAs in Arabidopsis thaliana infected with tobacco mosaic virus. *DNA Res*. **14**(5): 227–233.

Terrier, N., Glissant, D., Grimplet, J., Barrieu, F., Abbal, P., Couture, C., Ageorges, A., Atanassova, R., Leon, C., Renaudin, J. P., Dédaldéchamp, F., Romieu, C., Delrot, S. and Hamdi, S. (2005) Isogene specific oligo arrays reveal multifaceted changes in gene expression during grape berry (Vitis vinifera L.) development. *Planta*. **222**: 832-847. 10.1007/s00425-005-0017-y.

This, P., Lacombe, T. and Thomas, M. R. (2006) Historical origins and genetic diversity of wine grapes. *Trends Genet*. **22**:511-519.

Triantafilou, K., Vakakis, E., Kar, S., Richer, E., Evans, G. L. and Triantafilou, M. (2012) Visualisation of direct interaction of MDA5 and the dsRNA replicative intermediate form of positive strand RNA viruses. *J. Cell Sci*. **125**: 4761-4769.

Tsai, C-W., Chau, J., Fernandez, L., Bosco, D., Daane, K. M and Almeida, R. P. (2008) Transmission of grapevine leafroll-associated virus 3 by the vine mealybug (Planococcus ficus). *Phytopathology.* **98**:1093–1098. doi: 10.1094/PHYTO-98-10-1093.

Tsai, C. W., Daugherty, M. P. and Almaida, R. P. P. (2012) Seasonal dynamics and virus translation of grapevine leafroll-associated virus 3 in grapevine cultivars. *Plant Pathol.* **61**:977–985.

Varkonyi-Gasic, E., Wu, R., Wood, M., Walton, E. F. and Hellens, R. P. (2007) Protocol: a highly sensitive RT-PCR method for detection and quantification of microRNAs. *Plant Methods*. **3**(12).

Vega, A., Gutierrez, R. A., Pena-Neira, A., Cramer, G. R. and Arce-Johnson, P. (2011) Compatible GLRaV-3 viral infections affect berry ripening decreasing sugar accumulation and anthocyanin biosynthesis in Vitis vinifera. *Plant Mol Biol*. **77**:261–274.

Wallis, C. M., Wallingford, A. K. and Chen, J. (2013) Grapevine rootstock effects on scion sap phenolic levels, resistance to Xylella fastidiosa infection, and progression of Pierce's disease. *Front. Plant Sci.* **4**: 502. doi: 10.3389/fpls.2013.00502 PMID: 24376452.

Wang, J., Sharma, A. M., Duffy, S. and Almeida, R. P. P. (2011a) Genetic diversity in the 30 terminal 4.6-kb region of Grapevine leafroll associated virus 3. *Phytopathology*. **101**: 445–450.

Wang, J. -W., Park, M. Y., Wang, L. -J., Koo, Y., Chen, X. -Y., Weigel, D. and Poethig, R. (2011b) miRNA control of vegetative phase transition in trees. *PLoS Genet*. **7**: e1002012.

Wark, A. W., Lee, H. J. and Corn, R. M. (2008) Multiplexed detection methods for profiling microRNA expression in biological samples. *Angew. Chem. Int. Edn Engl*. **47**: 644–652.

Weber, E., Golino, D. A., and Rowhani, A. (1993) Leafroll disease of grapevines. *Pract. Wine. Vineyard*. **14**: 21–24.

Zeng, C., Wang, W., Zheng, Y., Chen, X., Bo, W., Song, S., Zhang, W. and Peng, M. (2010) Conservation and divergence of microRNAs and their functions in Euphorbiaceous plants. *Nucleic Acids Res*. **38**:981–995.

Zhang, B., Pan, X., Cannon, C. H., Cobb, G. P. and Anderson, T. A. (2006) Conservation and divergence of plant microRNA genes. *Plant J.* **46**:243–259.

Zhang, B., Pan, X. and Stellwag, E. J. (2008) Identification of soybean microRNAs and their targets. *Planta.* **229**:161–182.

Zhang, W., Gao, S., Zhou, X., Chellappan, P., Chen, Z., Zhou, X., Zhang, X., Fromuth, N., Coutino, G., Coffrey, M. and Jin, H. (2011) Bacteria-responsive microRNAs regulate plant innate immunity by modulating plant hormone networks. *Plant Mol. Biol*. **75**:93–105.

Zhang, Y. (2005) miRU: an automated plant miRNA target prediction server. *Nucleic Acids Res*. doi: 10.1093/nar/gki383.

Zhu, C., Ding, Y., and Liu, H. (2011) MiR398 and plant stress responses. *Physiol. Plant.* **143**:1–9. doi: 10.1111/j.1399-3054.2011.01477.x.

Addenda:

Addendum A Primers for miRNA stem-loop RT-qPCR and miRNA target RT-qPCR assays.

Primer	Sequence	Amp*	Target	Prim. Conc. [a]	T[A][b]	Ref.
miR408_UPL_RT	GTTGGCTCTGGTGCAGGGTCCGAGGTATTCGCACCAGAGCCAACGCCAGG	± 60	Vitis vinifera miR408	1	60	This Study
vvi-miR408_F	CGC CGT ATG CAC TGC CTC TTC			0.5-0.6		
miR399e-UPL	GTTGGCTCTGGTGCAGGGTCCGAGGTATTCGCACCAGAGCCAACCGGGC	± 60	Vitis vinifera miR399e	1	60	This Study
miR399e-forward	CGCCGCTGCCAAAGGAGATTT			0.5-0.6		
vvi-miR398b_UPL_RT	GTTGGCTCTGGTGCAGGGTCCGAGGTATTCGCACCAGAGCCAACCAGGGG	± 60	Vitis vinifera miR398b	1	60	This Study
vvi-miR398b_F	GGG GCT GTG TTC TCA GGT CG			0.5-0.6		
vvi-miR397a_UPL_RT	GTTGGCTCTGGTGCAGGGTCCGAGGTATTCGCACCAGAGCCAACCATCAA	± 60	Vitis vinifera miR397a	1	60	This Study
vvi-miR397a_F	CTG CCG TCA TTG AGT GCA GCG			0.5-0.6		
vvi-miR156g_UPL_RT	GTTGGCTCTGGTGCAGGGTCCGAGGTATTCGCACCAGAGCCAACGTGCTC	± 60	Vitis vinifera miR156g	1	60	This Study
vvi-miR156g_F	GTC CGC CCG TTG ACA GAA GAT AGA			0.5-0.6		
vvi-miR162_UPL_RT	GTTGGCTCTGGTGCAGGGTCCGAGGTATTCGCACCAGAGCCAACCTGGAT	± 60	Vitis vinifera miR162	1	60	This Study
vvi-miR162_F	GCC GTG GTC GAT AAA CCT CTG C			0.5-0.6		
vvi-miR166h_UPL_RT	GTTGGCTCTGGTGCAGGGTCCGAGGTATTCGCACCAGAGCCAACGGGGAA	± 60	Vitis vinifera miR166h	1	60	This Study
vvi-miR166h_F	TAC GCT CGG ACC AGG CTT CA			0.5-0.6		
vvi-miR393a_UPL_RT	GTTGGCTCTGGTGCAGGGTCCGAGGTATTCGCACCAGAGCCAACGATCAA	± 60	Vitis vinifera miR393a	1	60	This Study
vvi-miR393a_F	GCA ACT GTC CAA AGG GAT CGC A			0.5-0.6		
vvi-miR164a_UPL_RT	GTTGGCTCTGGTGCAGGGTCCGAGGTATTCGCACCAGAGCCAACTGCACG	± 60	Vitis vinifera miR164a	1	60	This Study
vvi-miR164a_F	GGG TGG AGA AGC AGG GCA			0.5-0.6		
miRNA159c_UPL_RT	GTTGGCTCTGGTGCAGGGTCCGAGGTATTCGCACCAGAGCCAACTAGAGC	± 60	Vitis vinifera miR159c	1	60	This Study
miRNA159c forward primer	CGGCGGTTTGGATTGAAGGGA			0.5-0.6		
miRNA167a_UPL_RT	GTTGGCTCTGGTGCAGGGTCCGAGGTATTCGCACCAGAGCCAACCAGATC	± 60	Vitis vinifera miR167a	1	60	This Study
miRNA167a forward primer	TCGCGTGAAGCTGCCAGCAT			0.5-0.6		
UPL reverse primer	GTGCAGGGTCCGAGGT		Stem-loop RT primer	0.5	60	Varkonyi-Gasic et al. (2007)

Addendum A Continued from previous page

Primer	Sequence	Amp*	Target	Prim. Conc. [a]	TA[b]	Ref.
Vv_actin_F	CTTGCATCCCTCAGCACCTT	82	Vitis vinifera actin	0.4	55	Reid *et al.* (2006)
Vv_actin_R	TCCTGTGGACAATGGATGGA					
Vv_α-tubulin_F	CAGCCAGATCTTCACGAGCTT	119	Vitis vinifera α-Tubulin	0.4	55	Reid *et al.* (2006)
Vv_α-tubulin_R	GTTCTCGCGCATTGACCATA					
Vv_UBC_F	GAGGGTCGTCAGGATTTGGA	75	Vitis vinifera UBC	0.4	55	Reid *et al.* (2006)
Vv_UBC_R	GCCCTGCACTTACCATCTTTAAG					
Vv_GAPDH_F	TTCTCGTTGAGGGCTATTCCA	70	Vitis vinifera GAPDH	0.4	55	Reid *et al.* (2006)
Vv_GAPDH_R	CCACAGACTTCATCGGTGACA					
Vv_EF1α_F	GAACTGGGTGCTTGATAGGC	150	Vitis vinifera EF1-α	0.4	55	Terrier *et al.* (2005)
Vv_EF1α_R	AACCAAAATATCCGGAGTAAAAGA					
miR408_Target.F	GCAGTTCTAGAGAAGAGGAAGTG	126	rRNA processing isoform 1	0.4	58	This study
miR408_Target.R	AGGCTGTCTCAGATGAATTTGG					
miR398b_Target.F	CTGATAGGCTACTGTGCTGATG	95	Serine-threonine-protein inase pbs1	0.4	58	This study
miR398b_Target.R	GGTGGAAGATCAAGAAGGTGAT					
miR397a_Target1.F	CCTGTTGAGCGGAACACTAT	85	Laccase-4-like enzyme	0.4	58	This study
miR397a_Target1.R	TGAACCAAACTCCTGGATTATCT					
miR164a_Target.F	CAAACAGCAAAGAATGAATGGGT	131	Nac domain-containing protein 100	0.4	58	This study
miR164a_Target.R	GGTGGCAGAACAGAAGGATT					
miR393a_Target1.F	GCGGCTATGGGTACTTGATT	114	Protein transport inhibitor response	0.4	58	This study
miR393a_Target1.R	CCCTCCATGTCATATGGTTCAG					
miR393a_Target2(2)_F	CTGCACATCACTAGTCTCCTTG	85	Protein auxin signalling f-box 2 like	0.4	58	This study
miR393a_Target2(2)_R	ACATCTTGCCACCAGTCTTT					
miR166h_Target.F	ACTTCTGGTTGCTCCGTTATAC	105	Homeobox-leucine zipper protein ATHB-15	0.4	58	This study
miR166h_Target.R	GGCATACTTGGGCCATTCT					
miR399e_Target.F	GAGAAGCAGCGGATGAAGAA	94	Uncharacterised protein LOC100265752	0.4	58	This study
miR399e_Target.R	AAGAGGGATCGTCGATGTAGA					
miR162_Target(2)_F	TTTCCAGACTCACCTCTCTTAAAC	111	Disease resistance rpp13-like protein 1	0.4	58	This study
miR162_Target(2)_R	GGGAGGAGAGAGTTGTAGGAA					

67

Addendum A Continued from previous page

Primer	Sequence	Amp*	Target	Prim. Conc. [a]	TA[b]	Ref.
miR156g_Target1.F	ATCGAGCATCTGGTCTTGGA	140	Squamosa promotor-binding-like protein 9	0.4	58	This study
miR156g_Target1.R	GCTACTACCTTCATTGCCCTTG					
miR156g_Target2.F	AGCGTTGCTCCCTTTCTT	103	Squamosa promotor-binding-like protein 16	0.4	58	This study
miR156g_Target2.R	CCAAATCACTCAACCTCCCA					
T7 vector primer	TAATACGACTCACTATAGGG	±250	pGEM® T Easy Vector	0.4	55	
SP6 vector primer	TACGATTTAGGTGACACTATAG				55	

* Amplicon size in base pairs (bp). [a]Primer concentration in µM. [b]Annealing temperature (T_A) in °C.

Addendum B All putative miRNA targets predicted with psRNAtarget and annotated using Blast2GO.

Target accession	Target description	GO annotation*
		miR397a targets
GSVIVT01034003001	laccase-4-like	C:apoplast; F:copper ion binding; F:hydroquinone:oxygen oxidoreductase activity; P:glucuronoxylan metabolic process; P:xylan biosynthetic process; P:lignin catabolic process; P:oxidation-reduction process
GSVIVT01016512001	laccase-17	C:apoplast; F:copper ion binding; F:hydroquinone:oxygen oxidoreductase activity; P:lignin catabolic process; P:oxidation-reduction process
GSVIVT01025694001	laccase-11-like	C:cell wall; C:apoplast; F:copper ion binding; F:pectinesterase activity; F:aspartyl esterase activity; F:hydroquinone:oxygen oxidoreductase activity; P:cell wall modification; P:lignin catabolic process; P:oxidation-reduction process
GSVIVT01034139001	laccase 17	C:apoplast; F:copper ion binding; F:hydroquinone:oxygen oxidoreductase activity; P:lignin catabolic process; P:oxidation-reduction process
GSVIVT01016490001	laccase-17	C:apoplast; F:copper ion binding; F:hydroquinone:oxygen oxidoreductase activity; P:lignin catabolic process; P:oxidation-reduction process
GSVIVT01033192001	laccase-11-like	C:cell wall; C:apoplast; F:copper ion binding; F:pectinesterase activity; F:aspartyl esterase activity; F:hydroquinone:oxygen oxidoreductase activity; P:cell wall modification; P:lignin catabolic process; P:oxidation-reduction process
GSVIVT01024795001	laccase-4	C:apoplast; F:copper ion binding; F:hydroquinone:oxygen oxidoreductase activity; P:lignin catabolic process; P:oxidation-reduction process
GSVIVT01025077001	laccase-17-like	C:apoplast; F:copper ion binding; F:hydroquinone:oxygen oxidoreductase activity; P:lignin catabolic process; P:oxidation-reduction process
GSVIVT01034146001	laccase-17-like	C:apoplast; F:copper ion binding; F:hydroquinone:oxygen oxidoreductase activity; P:lignin catabolic process; P:oxidation-reduction process
GSVIVT01034040001	laccase-7-like	C:apoplast; F:copper ion binding; F:hydroquinone:oxygen oxidoreductase activity; P:lignin catabolic process; P:oxidation-reduction process
GSVIVT01025046001	laccase 17	C:apoplast; F:copper ion binding; F:hydroquinone:oxygen oxidoreductase activity; P:lignin catabolic process; P:oxidation-reduction process
GSVIVT01016513001	laccase-17	C:apoplast; F:copper ion binding; F:hydroquinone:oxygen oxidoreductase activity; P:lignin catabolic process; P:oxidation-reduction process

Addendum B Continued from previous page.

Target accession	Target description	GO annotation*
miR397a targets		
GSVIVT01034138001	laccase 17	C:apoplast; F:copper ion binding; F:hydroquinone:oxygen oxidoreductase activity; P:lignin catabolic process; P:oxidation-reduction process
GSVIVT01033501001	laccase 11	C:cell wall; C:apoplast; F:copper ion binding; F:pectinesterase activity; F:aspartyl esterase activity; F:hydroquinone:oxygen oxidoreductase activity; P:cell wall modification; P:lignin catabolic process; P:oxidation-reduction process
GSVIVT01018939001	laccase-11-like	C:cell wall; C:apoplast; F:copper ion binding; F:pectinesterase activity; F:aspartyl esterase activity; F:hydroquinone:oxygen oxidoreductase activity; P:cell wall modification; P:lignin catabolic process; P:oxidation-reduction process
GSVIVT01026349001	two-component response regulator arr22-like	C:cytoplasm; F:phosphohistidine phosphatase activity; P:phosphorelay signal transduction system; P:protein dephosphorylation; P:circadian rhythm; P:vernalization response
GSVIVT01017305001	probable polygalacturonase at3g15720	C:extracellular region; F:polygalacturonase activity; P:carbohydrate metabolic process; P:cell wall organization
GSVIVT01019707001	heat repeat-containing protein 6 isoform x1	C:vacuolar membrane
GSVIVT01035995001	probable monogalactosyldiacylglycerol chloroplastic	C:chloroplast inner membrane; F:carbohydrate binding; F:1,2-diacylglycerol 3-beta-galactosyltransferase activity; P:glycolipid biosynthetic process; P:response to wounding; P:response to fungus; P:jasmonic acid biosynthetic process; P:response to jasmonic acid; P:embryo development ending in seed dormancy; P:thylakoid membrane organization; P:lipid glycosylation
GSVIVT01033957001	phosphoinositide phospholipase c 2-like	C:intracellular; F:phosphatidylinositol phospholipase C activity; F:signal transducer activity; P:lipid catabolic process; P:intracellular signal transduction
miR408 targets		
GSVIVT01028654001	basic blue	F:electron carrier activity
GSVIVT01018246001	rrna processing isoform 1	C:nucleus
miR398b targets		
GSVIVT01000937001	serine threonine-protein kinase pbs1	C:plasma membrane; F:protein serine/threonine kinase activity; F:non-membrane spanning protein tyrosine kinase activity; F:ATP binding; P:pattern recognition receptor signaling pathway; P:defence response to bacterium, incompatible interaction; P:peptidyl-tyrosine phosphorylation; P:protein autophosphorylation

70

Addendum B Continued from previous page.

Target accession	Target description	GO annotation*
	miR393a targets	
GSVIVT01010995001	protein transport inhibitor response 1	C:SCF ubiquitin ligase complex; F:inositol hexakisphosphate binding; F:ubiquitin-protein transferase activity; F:auxin binding; F:auxin receptor activity; P:ubiquitin-dependent protein catabolic process; P:auxin-activated signaling pathway; P:stomatal complex morphogenesis; P:pollen maturation; P:lateral root formation; P:protein ubiquitination; P:regulation of circadian rhythm; P:stamen development
GSVIVT01021910001	protein transport inhibitor response 1	C:SCF ubiquitin ligase complex; F:inositol hexakisphosphate binding; F:auxin binding; F:auxin receptor activity; P:auxin-activated signaling pathway; P:pollen maturation; P:lateral root formation; P:stamen development
GSVIVT01033011001	protein auxin signaling f-box 2-like	F:inositol hexakisphosphate binding; P:auxin-activated signaling pathway
GSVIVT01031396001	nucleobase-ascorbate transporter 12	C:plasma membrane; F:adenine transmembrane transporter activity; F:guanine transmembrane transporter activity; F:uracil transmembrane transporter activity; F:solute:cation symporter activity; P:hypoxanthine transport; P:cation transmembrane transport; P:adenine import across plasma membrane; P:guanine import across plasma membrane; P:uracil import across plasma membrane
GSVIVT01013697001	unnamed protein product	C:vacuole
GSVIVT01031516001	abc transporter g family member 3-like	C:plasma membrane; F:ATP binding; F:maltose-transporting ATPase activity; P:metabolic process; P:maltose transport
	miR166h targets	
GSVIVT01035612001	Homeobox leucine zipper ATHB-15	C:nucleus; F:DNA binding; P:positive regulation of cell proliferation; P: primary shoot apical meristem specification; F:lipid binding; P:positive regulation of cell differentiation; P:xylem development
	miR162 targets	
GSVIVT01027229001	disease resistance rpp13-like protein 1	F:ADP binding
GSVIVT01027270001	disease resistance rpp13-like protein 1	F:ADP binding
GSVIVT01010700001	disease resistance rpp13-like protein 1	F:ADP binding
GSVIVT01027276001	disease resistance rpp13-like protein 1	F:ADP binding
	miR156g targets	
GSVIVT01010496001	squamosa promoter-binding-like protein 2 isoform x1	C:nucleus; F:DNA binding
GSVIVT01033519001	squamosa promoter-binding-like protein 9	C:nucleus; F:DNA binding

Addendum B Continued from previous page.

Target accession	Target description	GO annotation*
		miR156g targets
GSVIVT01032239001	squamosa promoter-binding-like protein 12 isoform x1	C:nucleus; F:DNA binding
GSVIVT01012247001	squamosa promoter-binding-like protein 6 isoform x1	C:nucleus; F:DNA binding
GSVIVT01010522001	squamosa promoter-binding-like protein 16	C:nucleus; F:DNA binding
GSVIVT01018205001	squamosa promoter-binding-like protein 7	C:nucleus; F:DNA binding
GSVIVT01008556001	squamosa promoter-binding-like protein 13a	C:nucleus; F:DNA binding
GSVIVT01033064001	squamosa promoter-binding-like protein 16	C:nucleus; F:DNA binding
GSVIVT01009602001	cytochrome p450 cyp82d47-like	F:monooxygenase activity; F:iron ion binding; F:oxidoreductase activity, acting on paired donors, with incorporation or reduction of molecular oxygen; F:heme binding; P:oxidation-reduction process
GSVIVT01008191001	calcium-dependent phosphotriesterase superfamily	F:strictosidine synthase activity; P:biosynthetic process
GSVIVT01016962001	probable disease resistance protein at5g63020	F:ATP binding; F:ADP binding
		miR164a targets
GSVIVT01007982001	nac domain-containing protein 100	C:nucleus; F:DNA binding; P:transcription, DNA-templated; P:regulation of transcription, DNA-templated
GSVIVT01014287001	protein cup-shaped cotyledon 2	C:nucleus; F:DNA binding; P:transcription, DNA-templated; P:regulation of transcription, DNA-templated
GSVIVT01020478001	nac domain-containing protein 21 22	C:nucleus; F:DNA binding; P:transcription, DNA-templated; P:regulation of transcription, DNA-templated
GSVIVT01019667001	growth-regulating factor isoform 1	P:cellular process
GSVIVT01016290001	aminodeoxychorismate chloroplastic isoform x1	F:oxo-acid-lyase activity; P:folic acid-containing compound biosynthetic process; P:dicarboxylic acid metabolic process

*GO annotations if available: C=Cellular component, F=Molecular function, P=Biological process.